LIMITING ACCURACY OF FOS WAVELENGTH CALIBRATION

R. BOHLIN, M. SIRK, and G. HARTIG
SPACE TELESCOPE SCIENCE INSTITUTE

Instrument Science Report CAL/FOS—044
October 1987

ABSTRACT

Analysis of new data indicates that the FOS internal calibration lamps produce spectra that are systematically offset from spectra of an external lamp which fully illuminates the spectrograph optics. Evidence is presented that these offsets are unstable and that uncertainties in the offsets may limit the accuracy of the wavelength calibration on orbit. Possible corrective measures are suggested.

I. Introduction

A previous report on the FOS wavelength calibration (Sirk and Bohlin 1986a) describes the method of performing wavelength calibrations utilizing the 0.1 arcsec apertures with the internal Pt-Cr-Ne calibration lamps. A later report, *FOS Entrance Aperture Offsets* (Sirk and Bohlin 1986b) describes a procedure to determine a wavelength scale of a science spectrum obtained through any aperture, assuming that the shift of spectral features between an internal Pt–Cr–Ne lamp and an external source is stable over time. The internal RMS error of an FOS wavelength calibration is typically 0.03 diode. However, an absolute wavelength scale will only be as accurate as the uncertainty in the internal/external offset. In the internal/external offset report (Sirk and Bohlin, 1987), non-constant offsets as large as 0.3 diode are observed for the red tube. In this paper, the temporal stability of these offsets is investigated as the expected limiting factor in the accuracy of FOS wavelengths for external astronomical sources. If the internal/external offsets change from the laboratory to orbit, the offsets will be difficult to derive, since the astronomical standard wavelength

objects do not have as high a density of clean lines as the external lamp that is used in the lab calibration. If the offset varies with time on orbit, then the offset will be even harder to establish.

II. Data and Analysis

In October of 1986, a special test was run on the FOS using the internal Pt–Cr–Ne lamps and an external Pt–Cr–Ne lamp for gratings G270H and G160L on the blue side, and G270H and G650L on the red side. The apertures were 0.1-Pair, 0.5-Pair, 1.0-Pair, 0.3 circular, and 1.0 circular on both sides. For a given grating and aperture combination, three spectra were obtained, one each from the two internal lamps and one from the external lamp without moving either the filter–grating wheel (FGW) or the aperture mechanisms. Thus, a shift in one spectrum relative to another cannot be ascribed to any lack of repeatability of the mechanisms.

The calibration procedure outlined in Sirk and Bohlin (1987) was performed in March, 1987 at LMSC for both the red and blue sides. The procedure was essentially the same as that of the 1986 test except that spectra from G190H, G400H, G570H, and G780H were obtained in addition to G270H. After the Digicon had been moved 0.4 mm away from the FGW, a subset of the above procedure was run on the red tube to test for spectral shifts as a function of focus.

For the 0.1-Pair, 0.25-Pair, 0.5-Pair, and the 0.3 circular apertures, spectral offsets are determined by comparing the measured line centroids of sharp, unblended spectral lines of one spectrum with the centroids of the same lines of another spectrum, as described in Sirk and Bohlin, 1986a, § IV.

III. Short Term Stability

To verify that the MgF_2 diffuser is providing uniform illumination of the apertures by the external lamp, the diffuser was rotated 180 degrees between two consecutive test exposures taken in March 1987. No spectral shift is detected to an accuracy of 0.02 diode.

G270H spectra obtained with the 0.1-Pair aperture were taken at the beginning and at the end of the program to investigate short term shifts. Figures 1a and 1b show the offsets between external Pt–Cr–Ne spectra for the red and blue tubes, respectively. The time difference between the spectra is 5 hours for the red tube and 3.5 hours for the blue tube. The offsets are constant and are due to Filter–Grating Wheel (FGW) non–repeatability (Hartig 1986) and/or a thermal shift. The maximum observed temperature change of the optical bench during the period in which all the data was obtained is 2 degrees C for the red tube in 1987. The average temperature is about 21 degrees C for both 1986 and 1987.

IV. Internal/External Offsets

The positions of spectral features of the external Pt–Cr–Ne lamp minus the positions of the internal direct lamp are shown as Figures 2a–h and 3a–h for the red and blue tube, respectively. In all eight plots of Figure 2, the red tube offsets are non-linear as a function of diode number and have a range of 0.3 diode. The shape of the offset curve is independent of the aperture or the grating to within 0.03 diode. However, on the blue tube the offsets are *not* independent of grating but still are independent of aperture. Gratings G400H and G570H (Figures 3g and 3h) on the blue side show zero offset, whereas gratings G190H and G270H (Figures 3a and 3f) show an offset with a total range of approximately 0.2 diode.

The magnitude of the offsets is dependent on the grating used for both tubes. Figures 4 and 5 summarize the external minus direct lamp offsets as a function of wavelength for the red and blue tubes, respectively.

V. Long Term Stability

Figures 6 and 7 show the external minus direct lamp offsets for the October 1986 data on G270H. On the red side, the internal/external offset is nearly 0.05 diode less in March 1987 than in Oct. 1986 at the lower diode numbers (cf. Figures 2a and 6). On the blue side, the offsets have dropped from just below zero in 1986 to about −0.1 diode in 1987 at the smaller diode numbers (cf. Figures 3a and 7).

In an attempt to understand this temporal instability, the change in line position from 1986 to 1987 for both the internal direct and cross-strapped lamps and for the external lamp are computed and displayed in Figures 8a–c for the red side and in Figures 9a–c for the blue side. On the red side, both internal lamps (Figures 8a–b) show identical changes with a small positive slope and a mean offset of −1.23 diodes. On the blue side, the internal lamps also show nearly identical changes, but with a larger, negative slope, and a mean offset of −0.75 diodes. The offset between Oct. 1986 and March 1987 may be attributed to the removal of side panels of the spectrograph enclosure just prior to the 1987 measurements. Image motion on the order of 100 microns is induced as a result of panel installation or removal, presumably due to stresses transferred from the enclosure to the optical bench.

The slopes seen in the comparisons of Figures 8 and 9 are indicative of changes in dispersion. This cannot be ascribed to changes in the grating or collimator tilt, since the variation in dispersion corresponding to the small (~ 1 diode) spectral offset is negligible. Rather, these effects are most likely due to motion of the detector relative to the focal plane. A simple geometrical calculation shows that slopes of the magnitude seen in Figures 8 and 9 can be produced by defocus motions on the order of 50 microns.

More difficult to understand are the opposite signs of the slopes for the blue side internal (Fig. 8a-b) and external (Fig. 8c) lamp offsets from 1986 to 1987. Focal plane changes cannot explain why the external spectral shifts differ from the internal shifts in the manner described above, even if the illumination of the gratings is non-uniform. However, a *change* in the illumination may serve to explain the difference in the offset slopes. When the FOS was opened for inspection in March 1987, the blue side was discovered to suffer from significant vignetting (~ 20%) of the f/24 beam by a bulge in the MLI blanket just below the grazing incidence mirror. This bulge was pulled back out of the beam before the measurements were made. If the illumination of the internal lamps was unaffected,

or affected differently from the external lamp illumination, by removal of this beam edge vignetting, relative shifts of ~ 0.1 diode could result.

VI. Offsets as a Function of Focus

FWHM are measured for approximately 10 well distributed spectral features on each of the gratings G190H, G270H, G400H, G570H, and G780H for the 1987 red tube data. FWHM are also measured for the data that were obtained after moving the red Digicon $\sim$0.4 mm away from the FGW for gratings G270H, G400H, and G570H. The internal/external offsets at the position of the measured spectral lines are plotted as a function of their measured FWHM in Figure 10. There is very strong correlation between FWHM and the magnitude of the internal/external offset for both the "normal" and "refocus" data. Since the refocusing caused certain lines to become narrow on one grating while simultaneously broadening lines on another grating, the gratings cannot be all co-focused. Furthermore, on G570H the lines at one end of the diode array remained at a constant width, while lines at the opposite end of the diode array increased in width by 0.2 diode! This result may be explained, if the digicon is tilted about a line perpendicular to both the optical axis and the dispersion direction. The expected FWHM of an emission line with a Gaussian profile that is out of focus by an amount Δf due to a tilt is

$$FWHM^2 = PSF^2 + \Delta f^2 = PSF^2 + \left(\frac{aTan\theta}{12}\right)^2$$

where PSF is the point spread function of a spectral line imaged by the $f/12$ gratings through the 0.1-Pair aperture, a is the distance in diodes along the diode array from the axis of rotation of the detector tilt, and θ is the detector tilt. Solving for θ and using values for the case of G570H mentioned above ($a = 500 diode, PSF = 0.3 diode, FWHM = 1.15 diode$) a tilt of about 1.5 degrees is obtained. Further analysis shows that the ranking of focus of the three gratings where data is available is G270H, G400H, G570H with the focus of grating G270H being the closest to the FGW. This analysis is rendered somewhat uncertain, however, by the fact that the actual effect of attempting to change the detector

focus position is somewhat indeterminate, since the detector mount does not lend itself well to this adjustment. It is possible that a fair amount of rotation about the X (dispersion) or Y (cross-dispersion) axis may have resulted.

VII. Discussion

The offsets between internal and external spectra seem to be dependent on focus and wavelength and independent of aperture. For the red tube, the fact that only the magnitude of the offset and not the shape of the offset curve changes as a function of wavelength suggests that the shape of the curve is due to a geometrical effect (*e.g.* a tilt). The red side direct calibration lamp illuminates only the edge of the gratings in the visual. Since the MgF_2 lens on the calibration lamps has the best focus at ~1500Å, a larger portion of the grating is illuminated in the UV than in the visual. Thus, the size and shape of an out of focus image may be dependent on wavelength.

The combination of a detector tilt, a change in the vignetting on the blue side , and a wavelength dependence of the shape of the asymmetric image produced by the internal lamps may account for the observed internal/external offsets.

VIII. Recommendations

The magnitude of the internal/external offsets is 0.3 diode on the red side and is an order of magnitude larger than the typical RMS wavelength calibration error. The lack of a precise specification for this offset may be the limiting factor in the accuracy of absolute wavelengths for external astronomical sources. Although the internal/external offsets can be determined as a function of diode number, the changes observed in the lab suggest that the offsets may be different after gravity release on orbit, and may not be stable. Furthermore, no offsets are likely to be measured in the lab in the far UV for G130H and G190H, since no additional vacuum testing is planned.

The logical approach to the offset problem is to eliminate its cause. The offsets may be minimized by installing the detectors with no tilt at the position of best compromise

focus. By measuring the FWHM of several lines at both ends of test spectra from all gratings, and by knowing the ranking of focus of the gratings, the best focus and zero tilt can be achieved. If the offsets do not vanish after careful installation of the detectors at their optimal positions, then adjustment of the calibration lamp transfer optics so that the gratings are fully illuminated remains the only means of ameliorating this problem.

References

Hartig, G. 1986, *Thermal Vacuum Measurements of the FOS Filter-Grating Wheel Repeatability* CAL/FOS-033, ST ScI.

Sirk, M., and Bohlin, R. 1986a, *FOS Wavelength Calibration* CAL/FOS–026, ST ScI.

Sirk, M., and Bohlin, R. 1986b, *FOS Entrance Aperture Offsets* CAL/FOS–029, ST ScI.

Sirk, M., and Bohlin, R. 1987, *Wavelength Offsets Among Internal Lamps and External Sources* CAL/FOS–041, ST ScI.

Figure Captions

The words pixel (px) and diode are used interchangably throughout this report.

Fig. 1– Demonstration of the stability of the spectral format over the short periods of 5 hours for the red tube (a) and 3.5 hours for the blue tube (b).

Fig. 2– Offsets on the red tube between the positions of spectral lines from an external lamp and from the internal direct lamp for various gratings and apertures for data obtained in March 1987.

Fig. 3– Same as Fig. 2, but for the blue side.

Fig. 4– Results of Fig. 2 summarized as a function of wavelength.

Fig. 5– Same as Fig. 4, but for the blue side.

Fig. 6– Same as Fig. 2a for data obtained in Oct 1986.

Fig. 7– Same as Fig. 3a for data obtained in Oct 1986.

Fig. 8– Offsets on the red tube between line positions for the 1986 and 1987 data for all 3 lamps on G270H.

Fig. 9– Same as Fig. 8, but for the blue side.

Fig. 10– Internal/External offsets as a function of line width for the red tube. The symbols are asterisk for G190H, triangle for G270H, diamond for G400H, square for G570H, and plus for G780H. Filled symbols are for a shift in focus of 0.4mm away from the FGW.

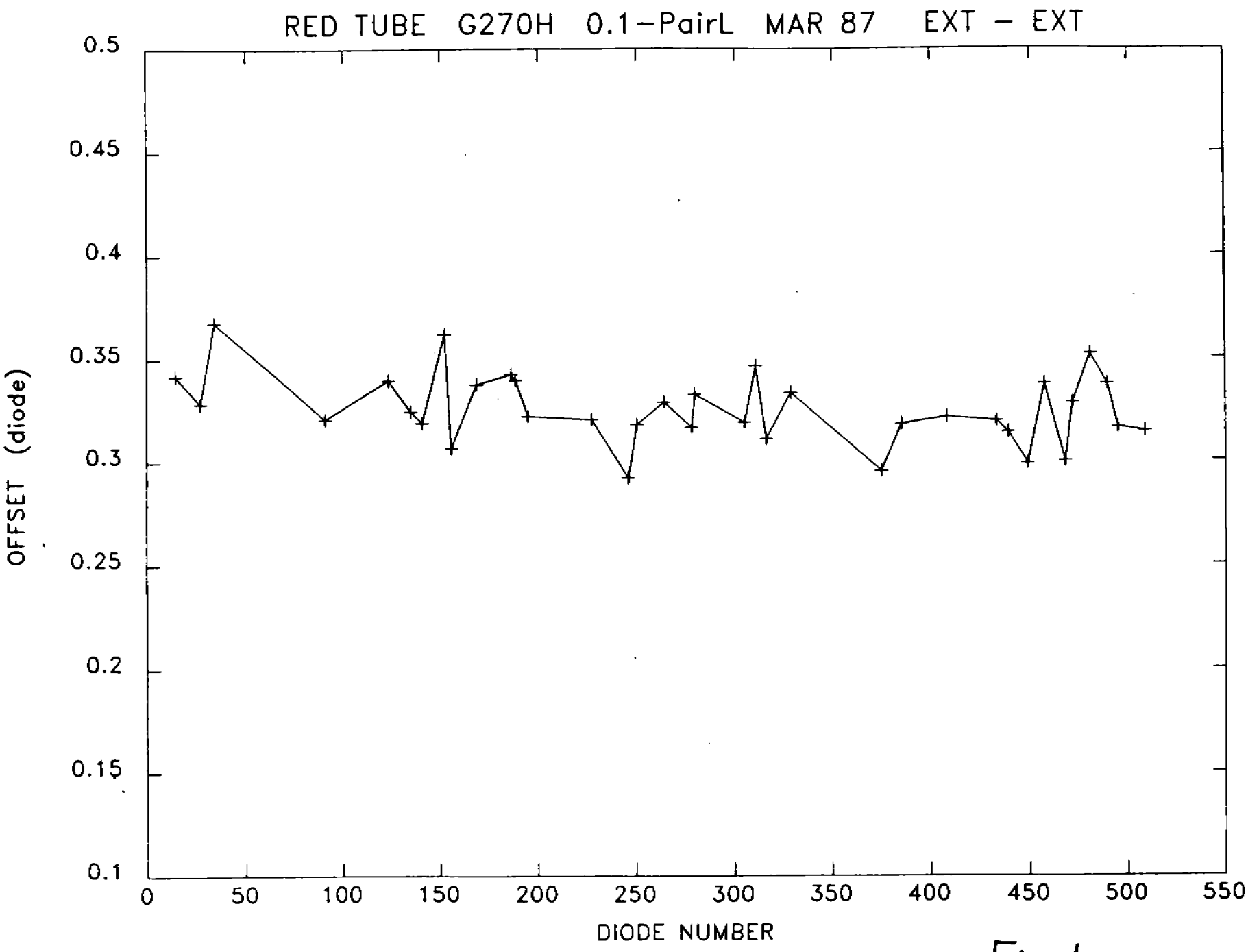
RED TUBE G270H 0.1-PairL MAR 87 EXT - EXT
OFFSET (diode)
0.5
0.45
0.4
0.35
0.3
0.25
0.2
0.15
0.1
0
50
100
150
200
250
300
350
400
450
500
550
DIODE NUMBER

Fig. 1a

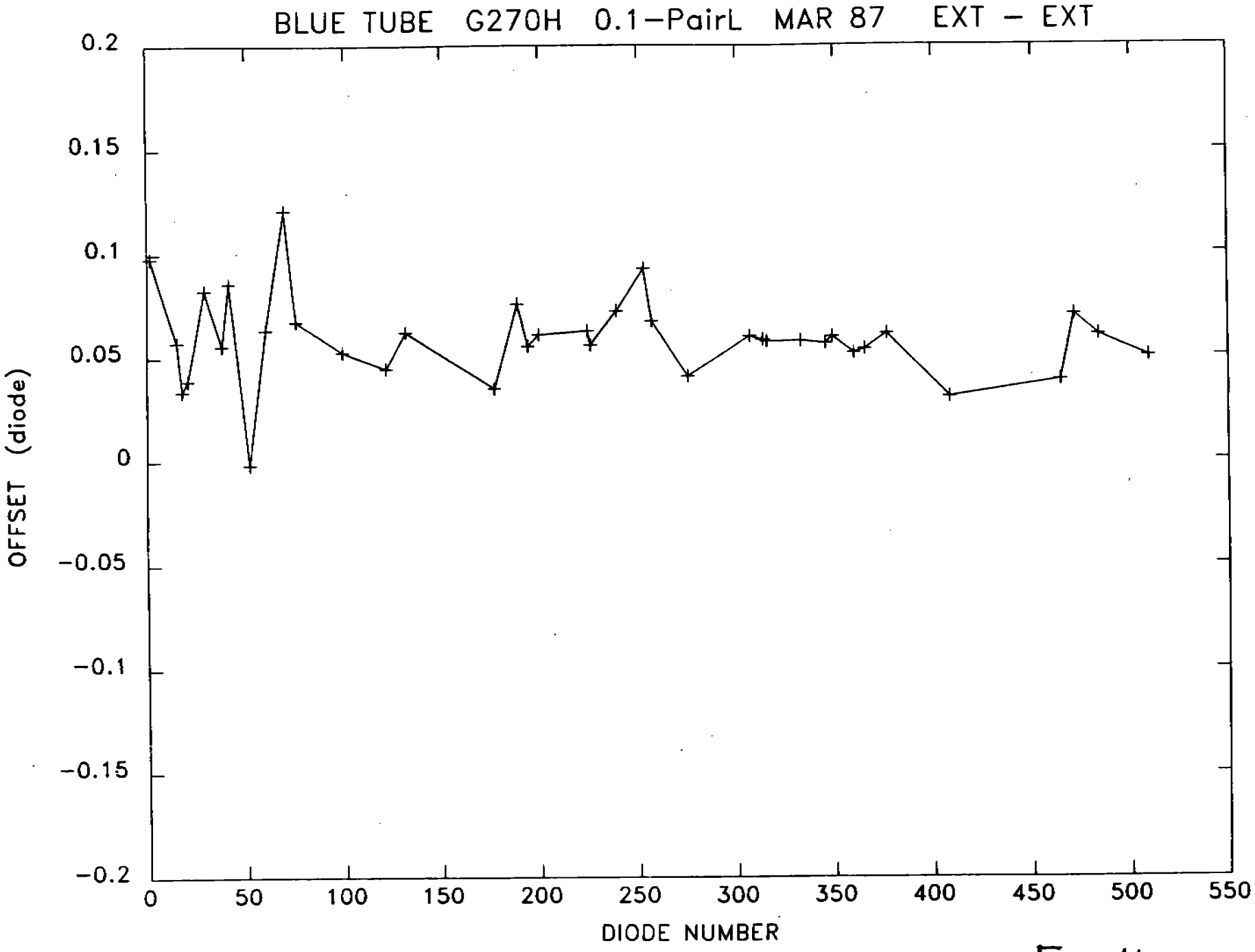
BLUE TUBE G270H 0.1–PairL MAR 87 EXT – EXT
0.2
0.15
0.1
0.05
0
−0.05
−0.1
−0.15
−0.2
OFFSET (diode)
0
50
100
150
200
250
300
350
400
450
500
550
DIODE NUMBER

Fig. 1b

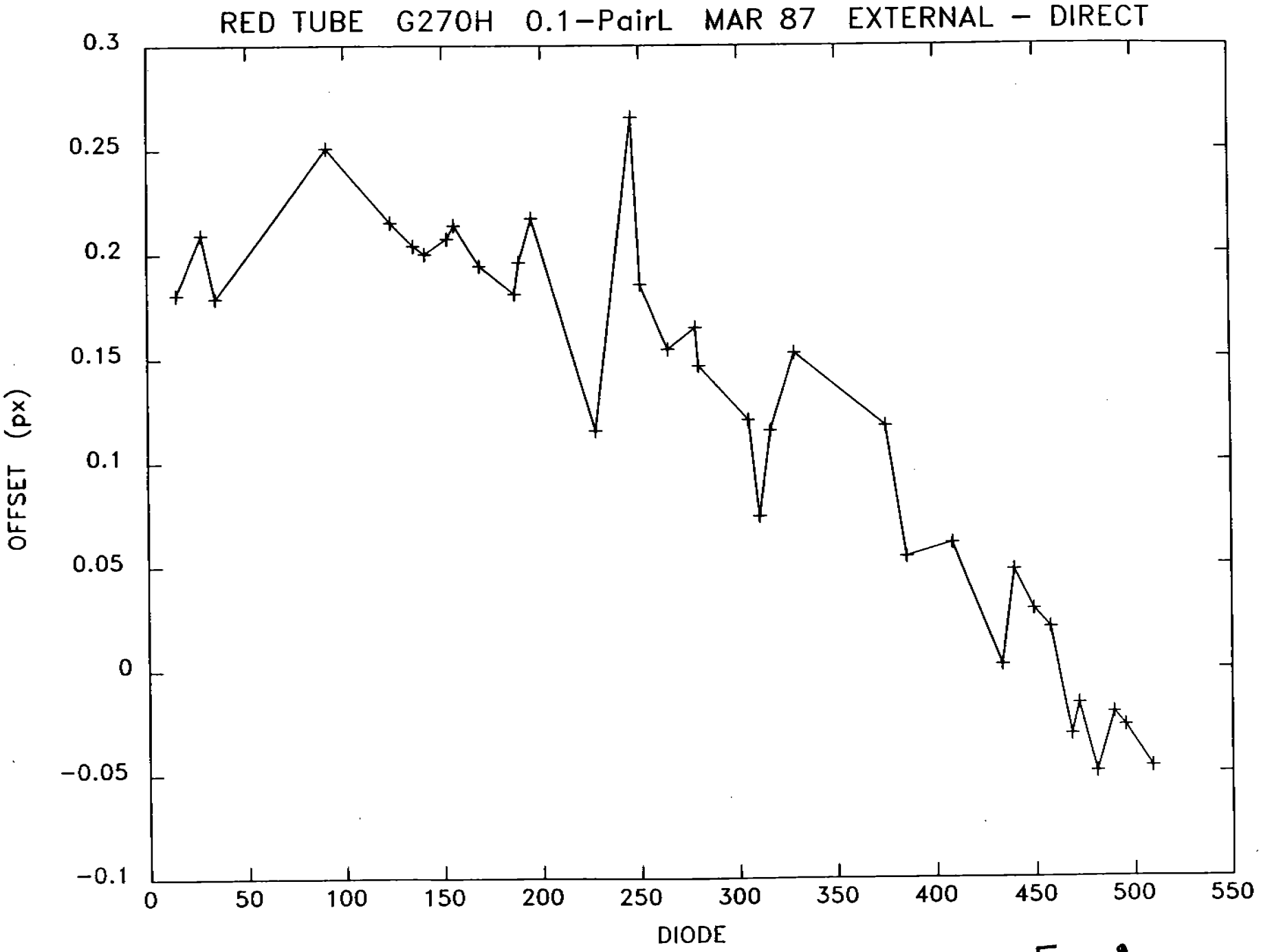
RED TUBE G270H 0.1-PairL MAR 87 EXTERNAL - DIRECT
OFFSET (px)
0.3
0.25
0.2
0.15
0.1
0.05
0
-0.05
-0.1
0
50
100
150
200
250
300
350
400
450
500
550
DIODE

Fig. 2a

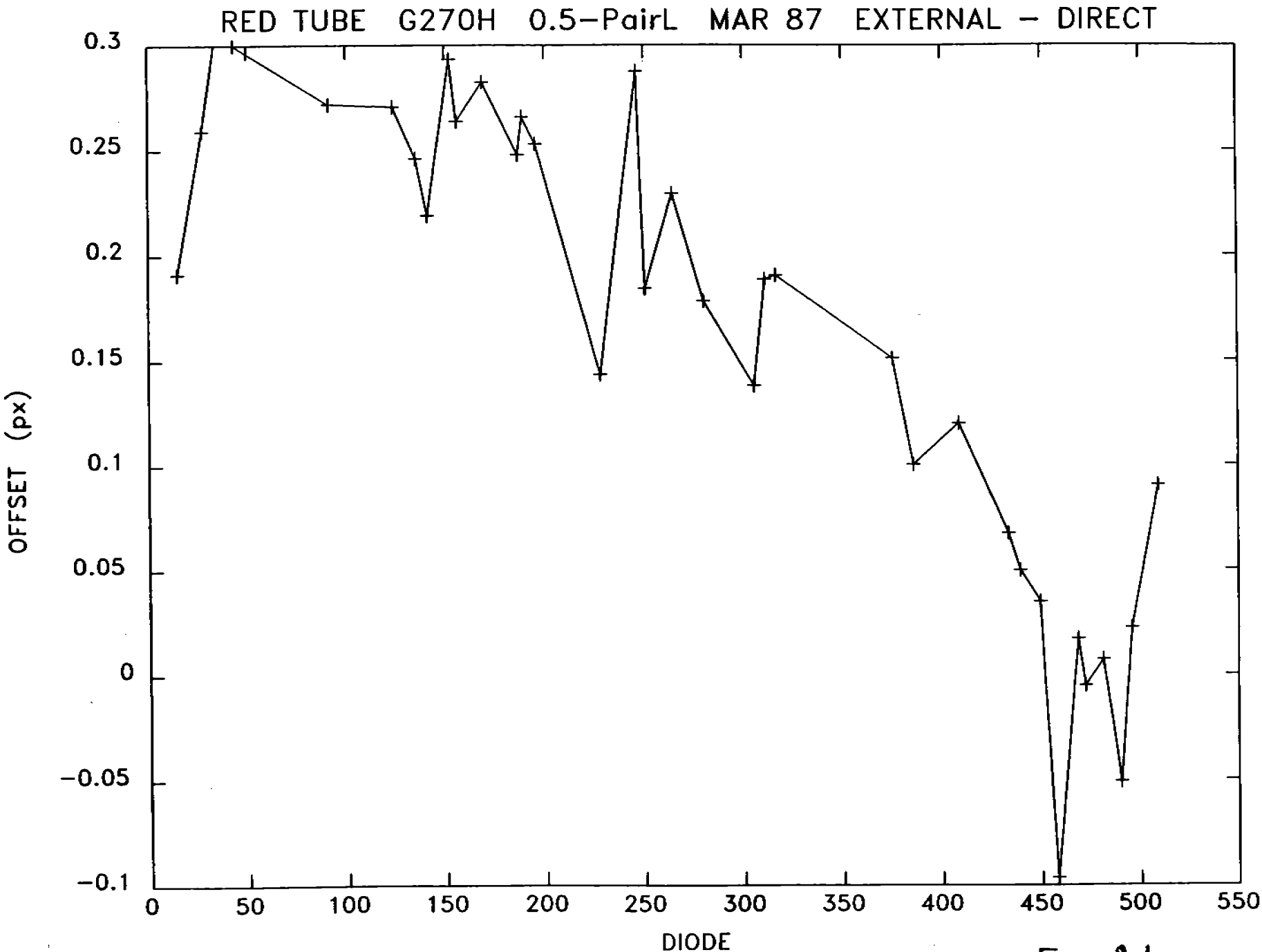
RED TUBE G270H 0.5-PairL MAR 87 EXTERNAL - DIRECT
OFFSET (px)
0.3
0.25
0.2
0.15
0.1
0.05
0
-0.05
-0.1
0
50
100
150
200
250
300
350
400
450
500
550
DIODE

Fig. 2b

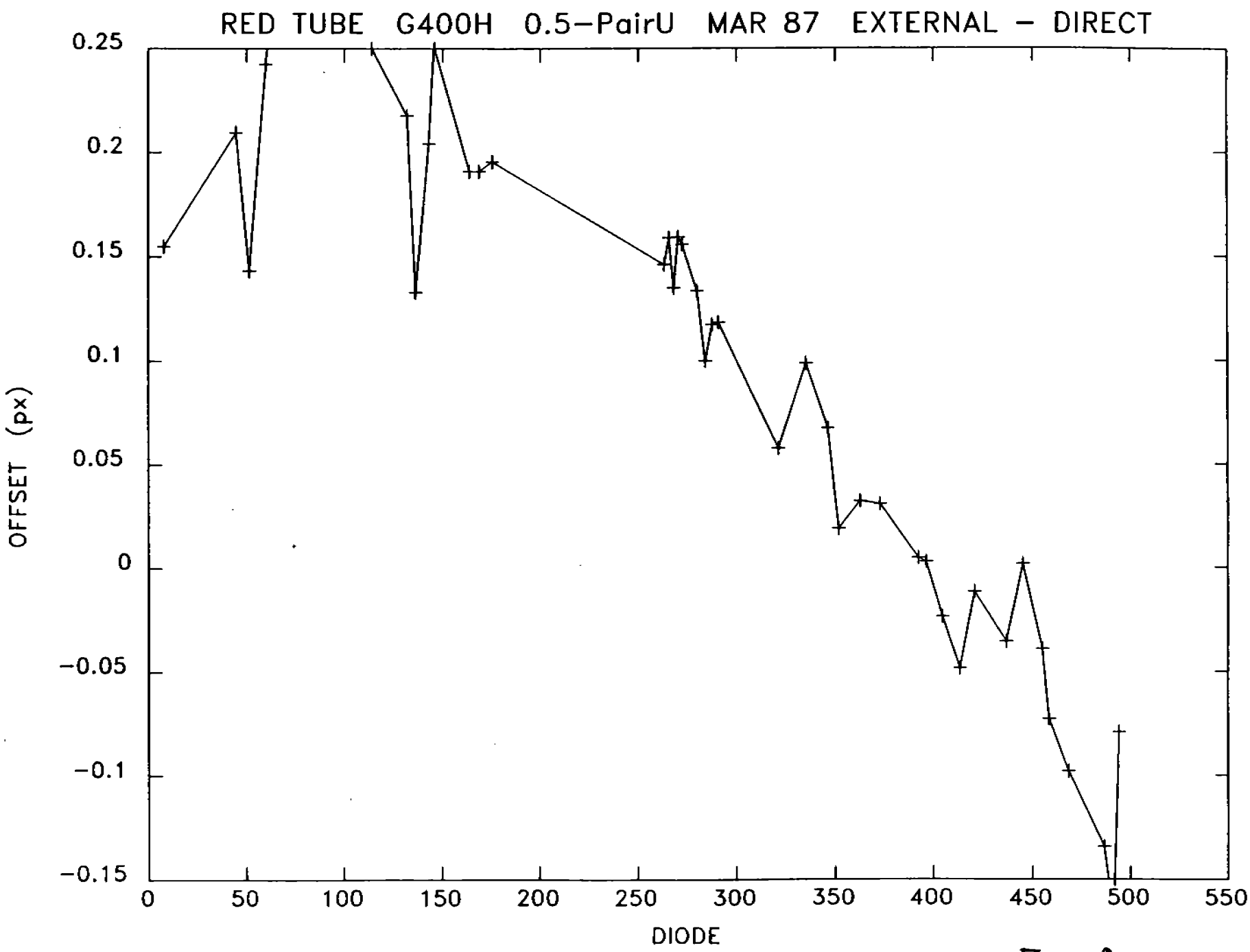
RED TUBE G400H 0.5–PairU MAR 87 EXTERNAL – DIRECT
0.25
0.2
0.15
0.1
0.05
0
−0.05
−0.1
−0.15
OFFSET (px)
0
50
100
150
200
250
300
350
400
450
500
550
DIODE

Fig. 2c

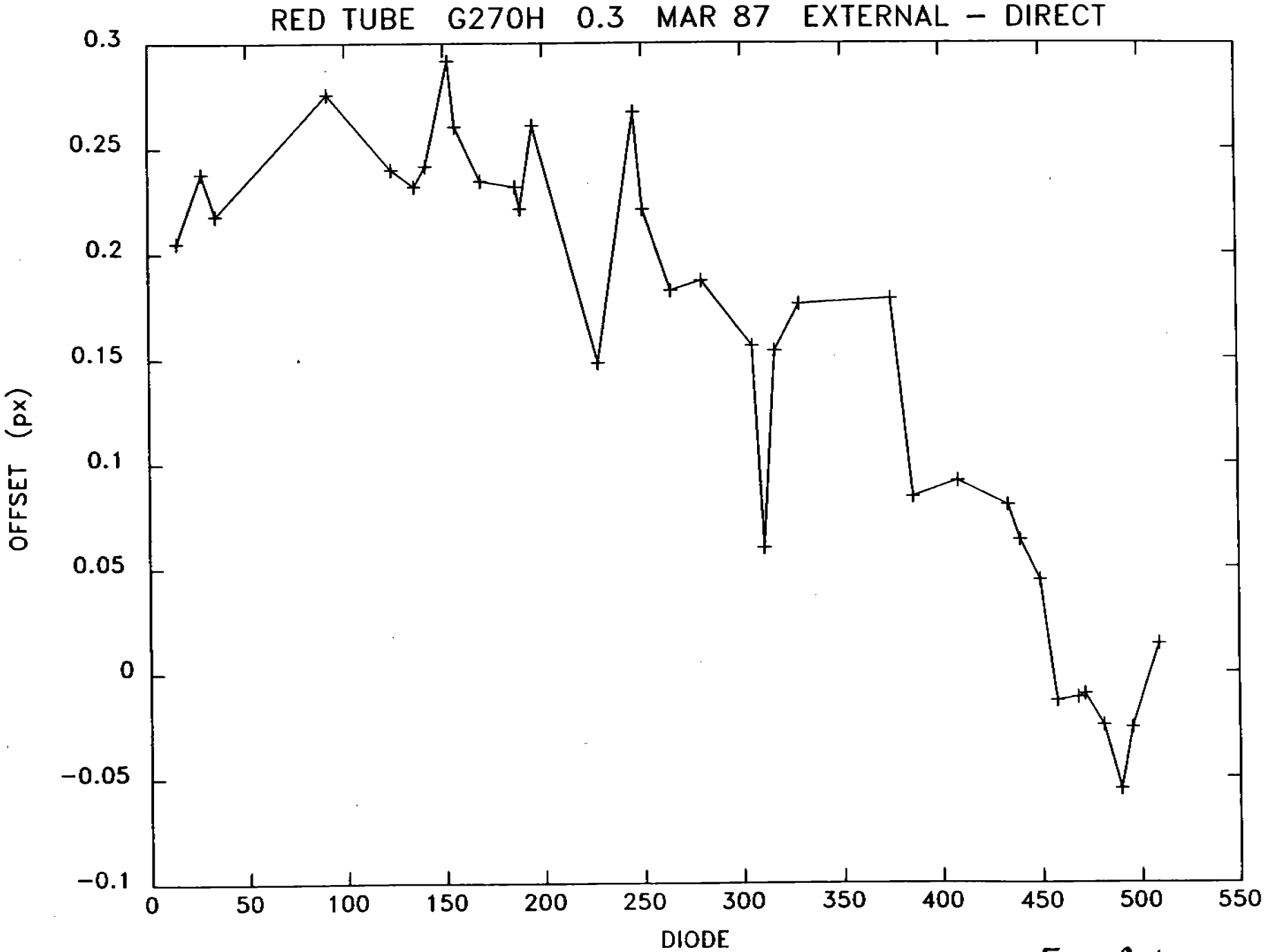
RED TUBE G270H 0.3 MAR 87 EXTERNAL – DIRECT
OFFSET (px)
0.3
0.25
0.2
0.15
0.1
0.05
0
−0.05
−0.1
0
50
100
150
200
250
300
350
400
450
500
550
DIODE

Fig. 2d

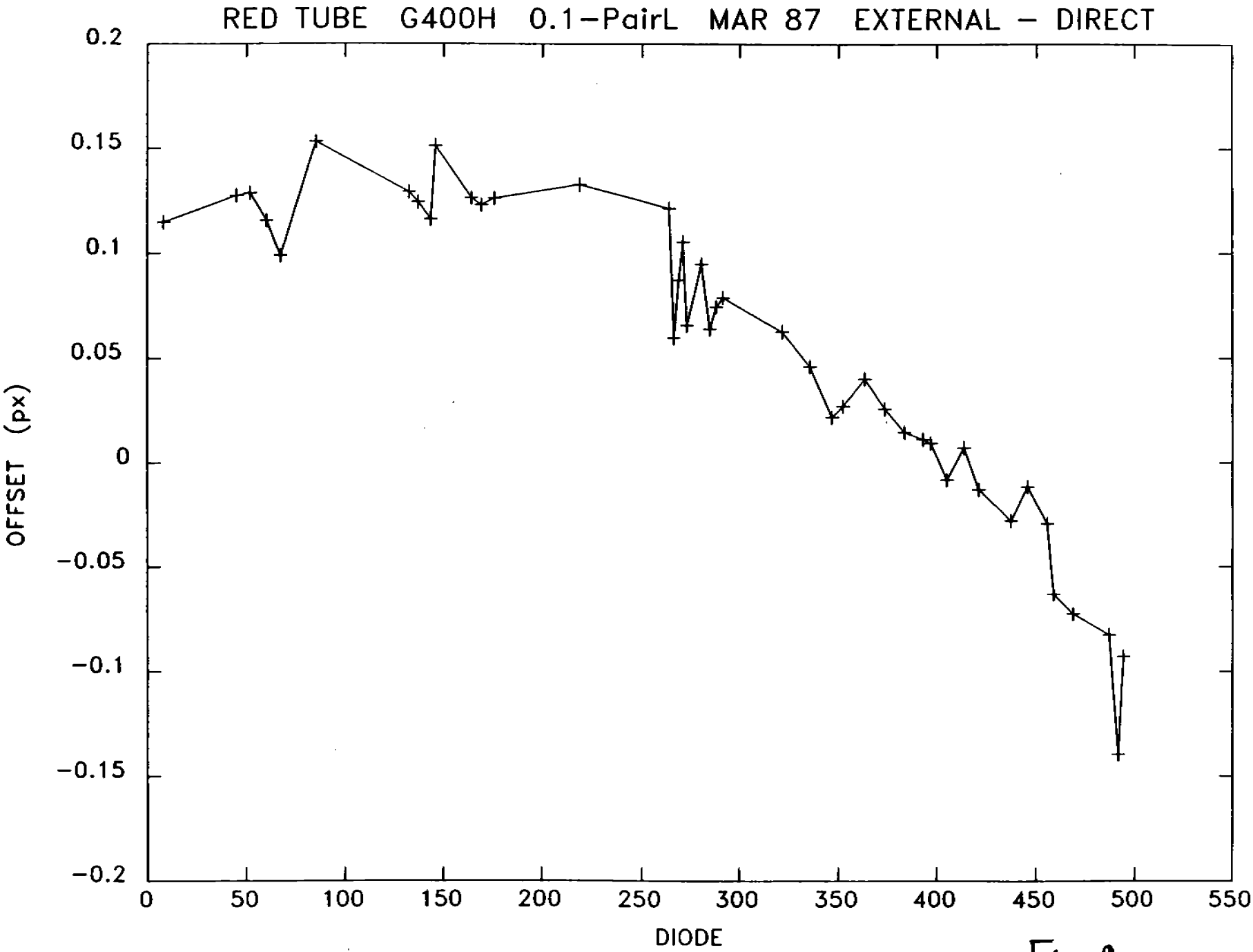
RED TUBE G400H 0.1-PairL MAR 87 EXTERNAL - DIRECT
0.2
0.15
0.1
0.05
0
-0.05
-0.1
-0.15
-0.2
OFFSET (px)
0
50
100
150
200
250
300
350
400
450
500
550
DIODE

Fig. 2e

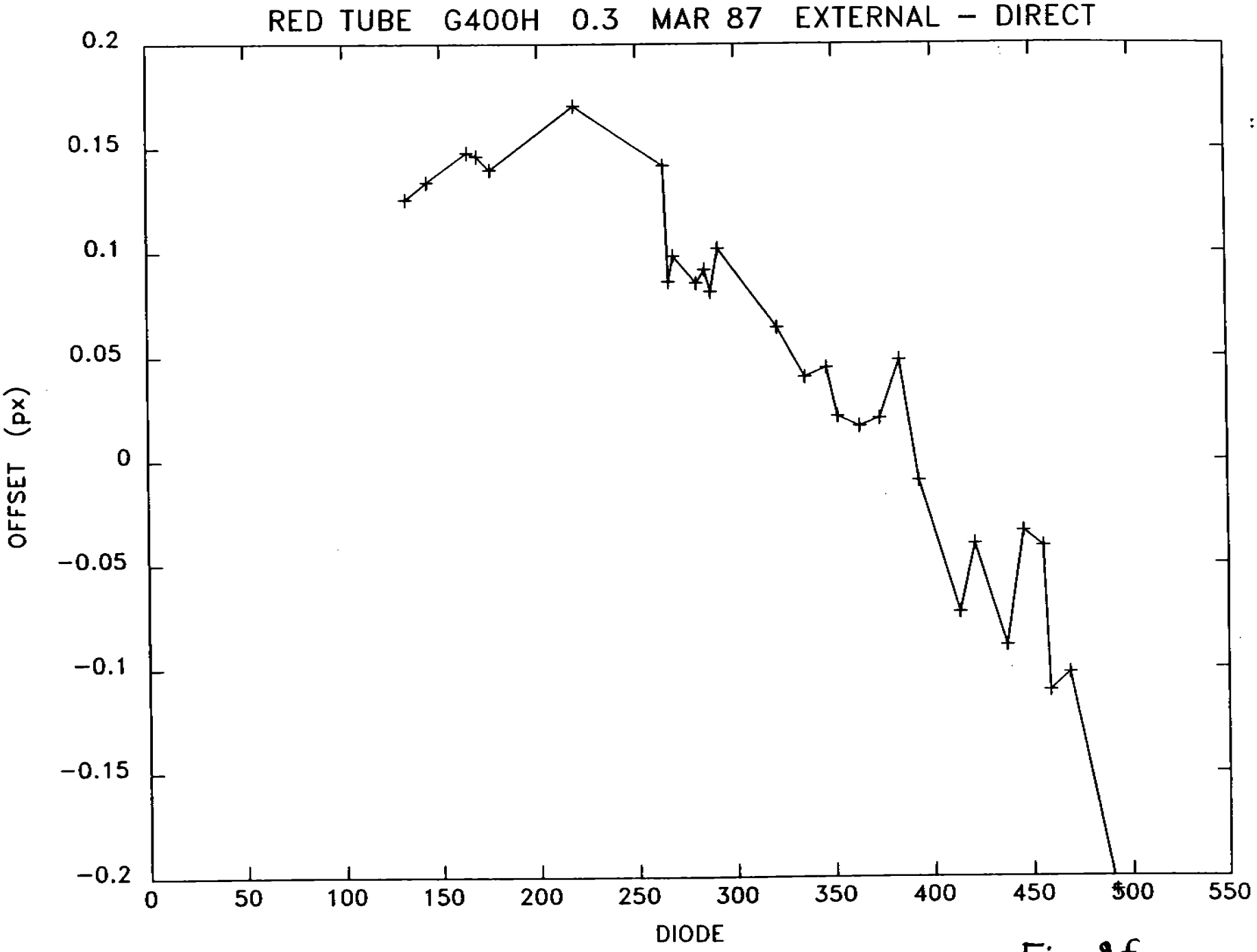
RED TUBE G400H 0.3 MAR 87 EXTERNAL – DIRECT
OFFSET (px)
0.2
0.15
0.1
0.05
0
−0.05
−0.1
−0.15
−0.2
0
50
100
150
200
250
300
350
400
450
500
550
DIODE

Fig. 2f

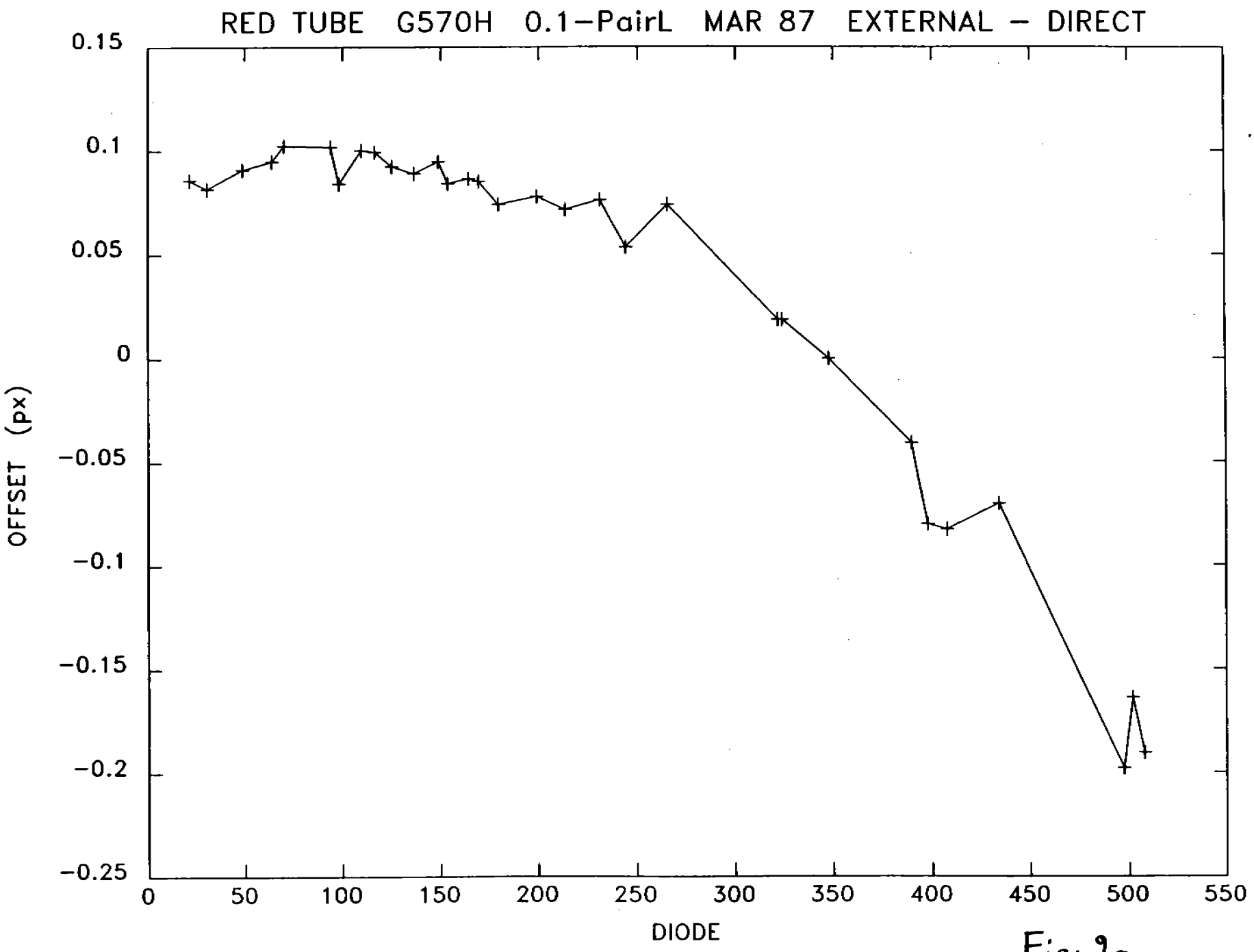
RED TUBE G570H 0.1-PairL MAR 87 EXTERNAL - DIRECT
0.15
0.1
0.05
0
-0.05
-0.1
-0.15
-0.2
-0.25
OFFSET (px)
0
50
100
150
200
250
300
350
400
450
500
550
DIODE

Fig. 2g

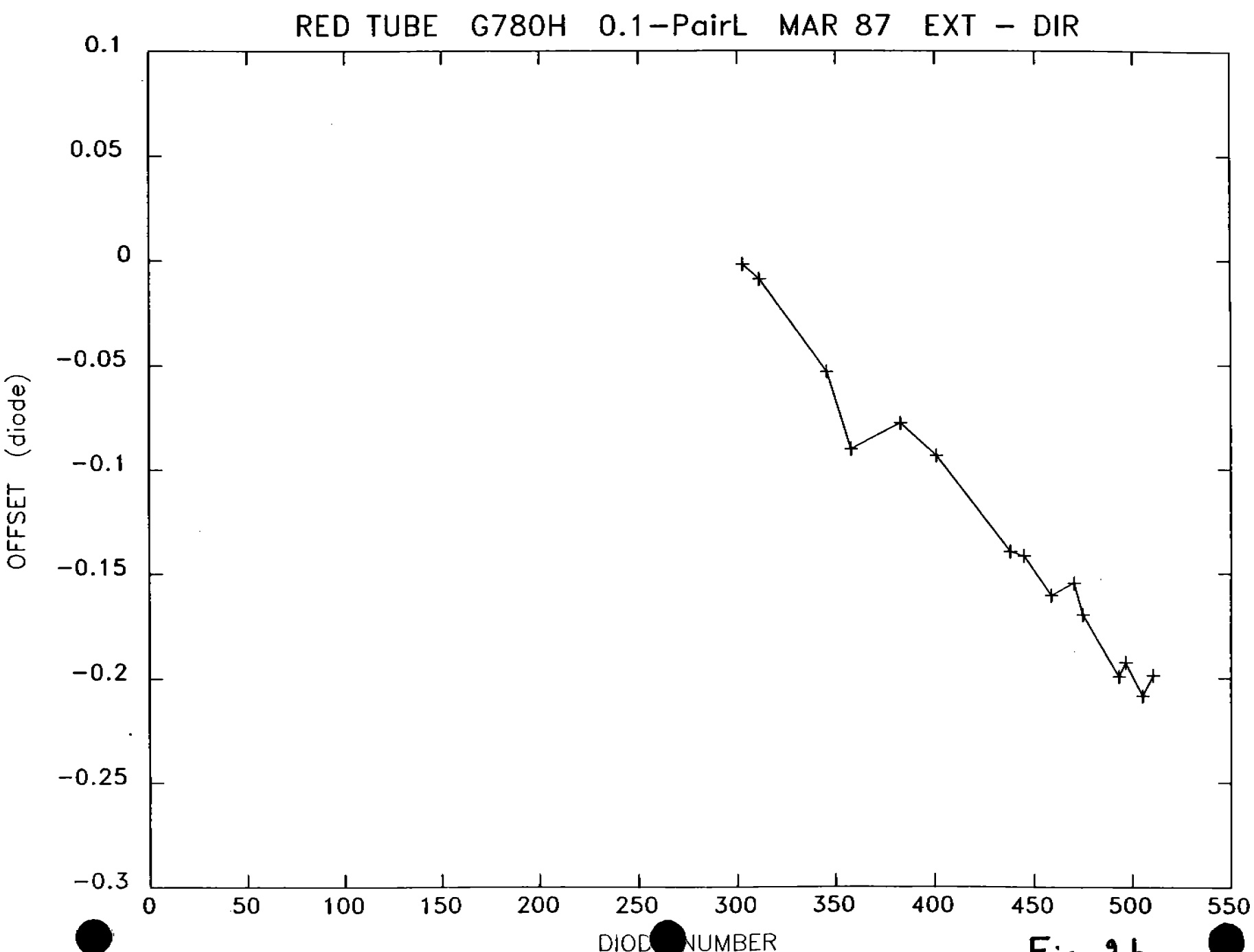
RED TUBE G780H 0.1-PairL MAR 87 EXT - DIR
0.1
0.05
0
-0.05
-0.1
-0.15
-0.2
-0.25
-0.3
OFFSET (diode)
0
50
100
150
200
250
300
350
400
450
500
550
DIODE NUMBER

0.1-Pair L

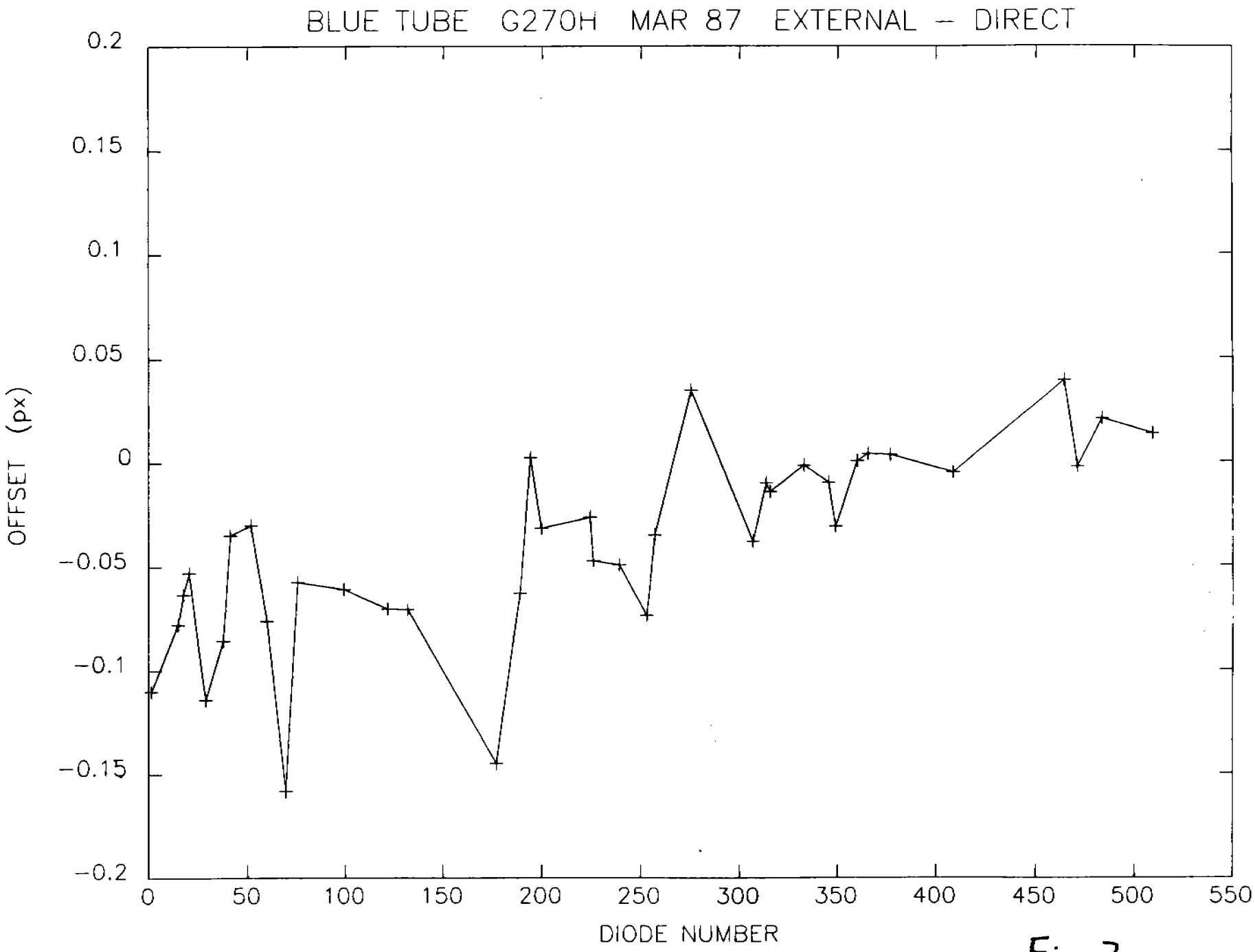

Fig. 3a

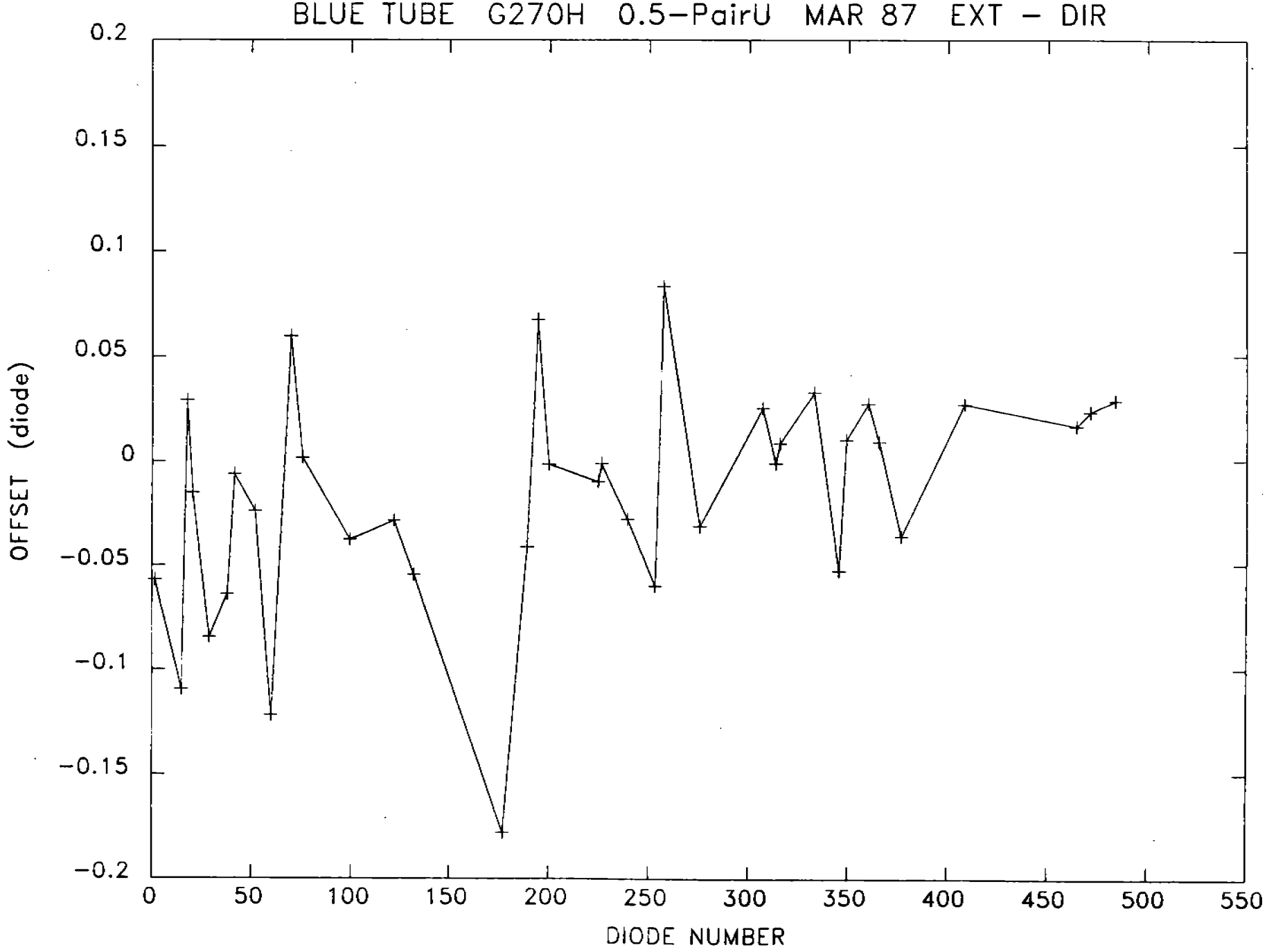
BLUE TUBE G270H 0.5–PairU MAR 87 EXT – DIR
OFFSET (diode)
DIODE NUMBER
0.2
0.15
0.1
0.05
0
−0.05
−0.1
−0.15
−0.2
0
50
100
150
200
250
300
350
400
450
500
550

Fig. 3b

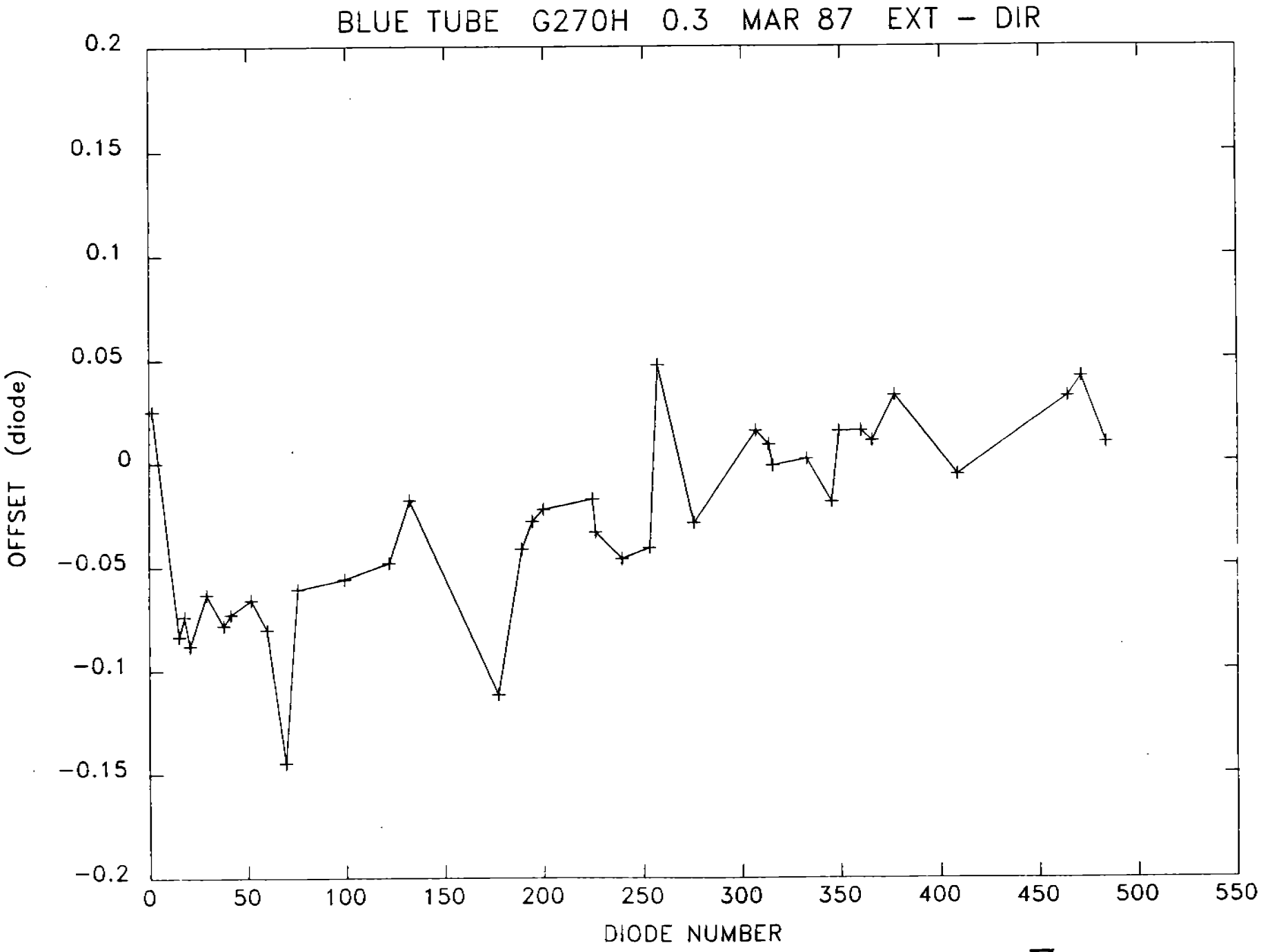
BLUE TUBE G270H 0.3 MAR 87 EXT – DIR
OFFSET (diode)
0.2
0.15
0.1
0.05
0
−0.05
−0.1
−0.15
−0.2
0
50
100
150
200
250
300
350
400
450
500
550
DIODE NUMBER

Fig. 3c

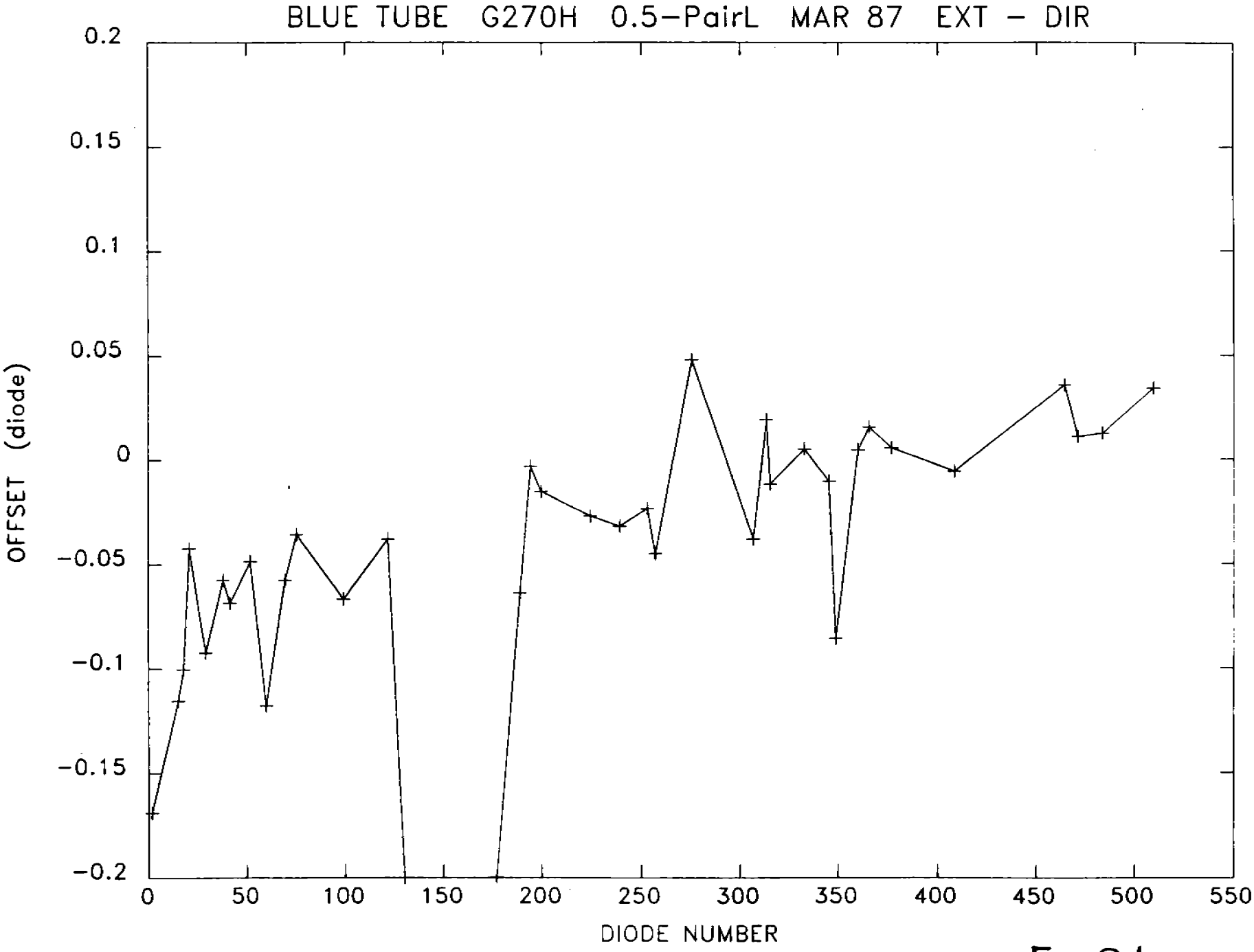
BLUE TUBE G270H 0.5-PairL MAR 87 EXT - DIR
OFFSET (diode)
DIODE NUMBER
0.2
0.15
0.1
0.05
0
-0.05
-0.1
-0.15
-0.2
0
50
100
150
200
250
300
350
400
450
500
550

Fig. 3d

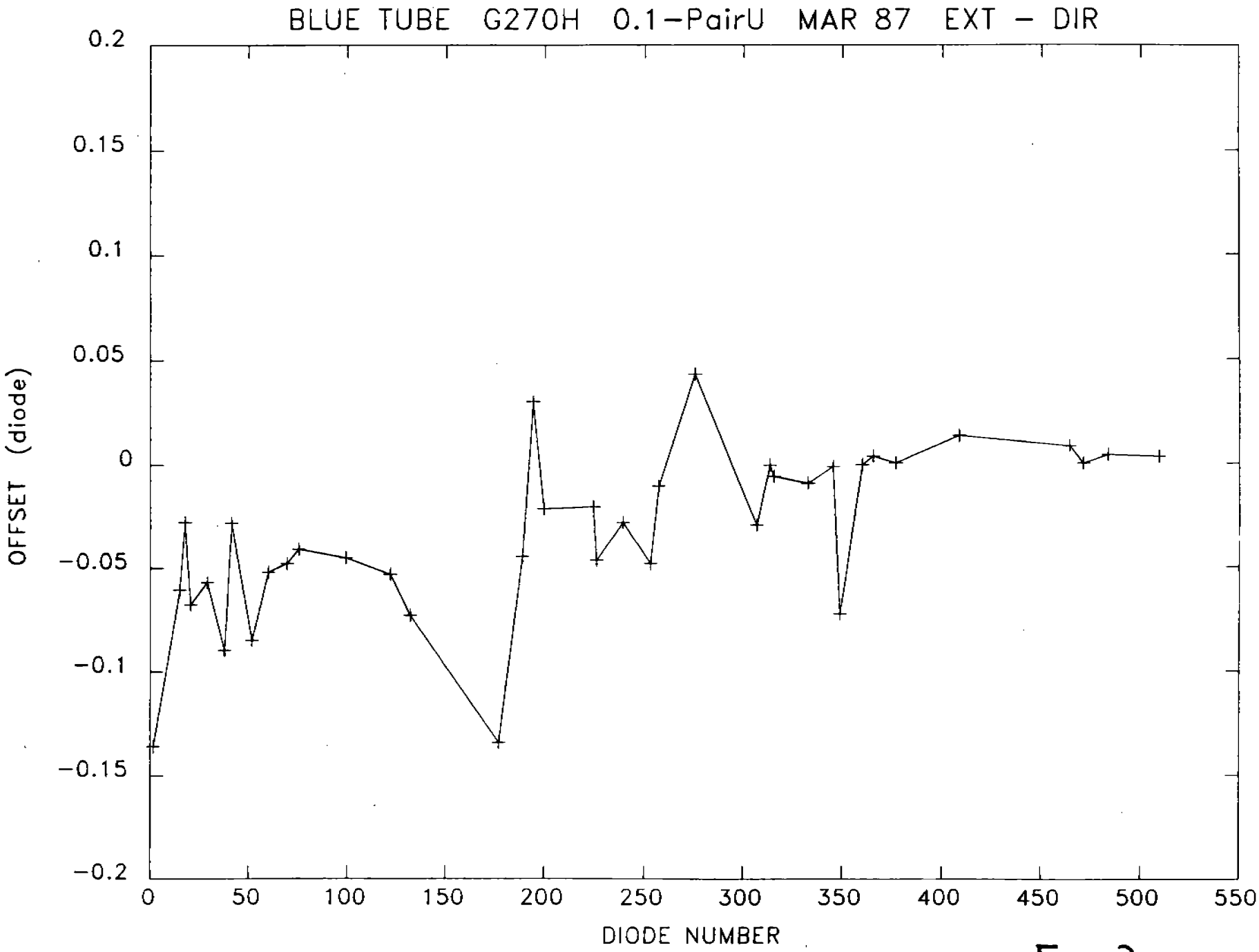
BLUE TUBE G270H 0.1-PairU MAR 87 EXT - DIR
0.2
0.15
0.1
0.05
0
-0.05
-0.1
-0.15
-0.2
OFFSET (diode)
0
50
100
150
200
250
300
350
400
450
500
550
DIODE NUMBER

Fig. 3e

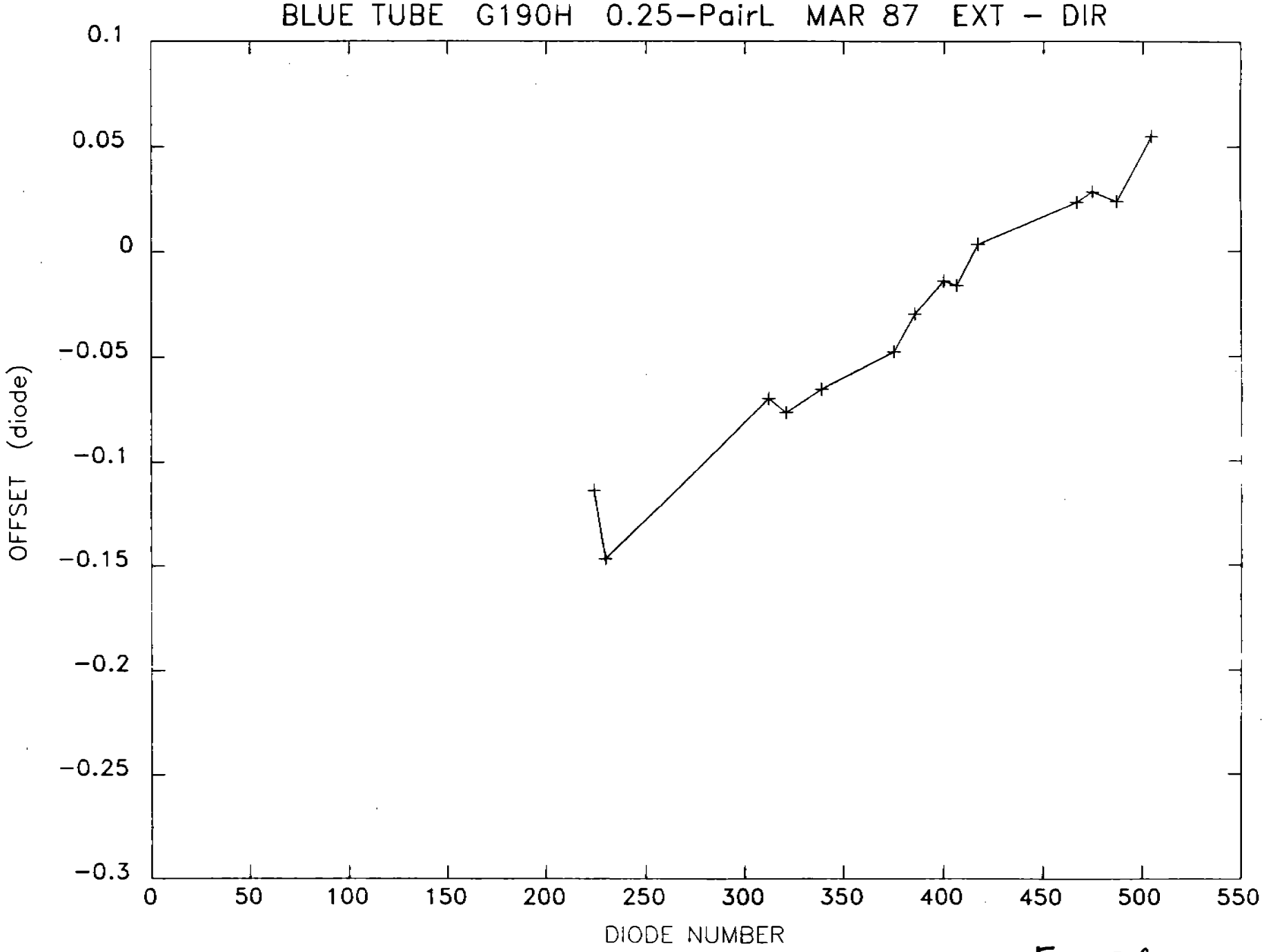
BLUE TUBE G190H 0.25-PairL MAR 87 EXT - DIR
0.1
0.05
0
-0.05
-0.1
-0.15
-0.2
-0.25
-0.3
OFFSET (diode)
0
50
100
150
200
250
300
350
400
450
500
550
DIODE NUMBER

Fig. 3f

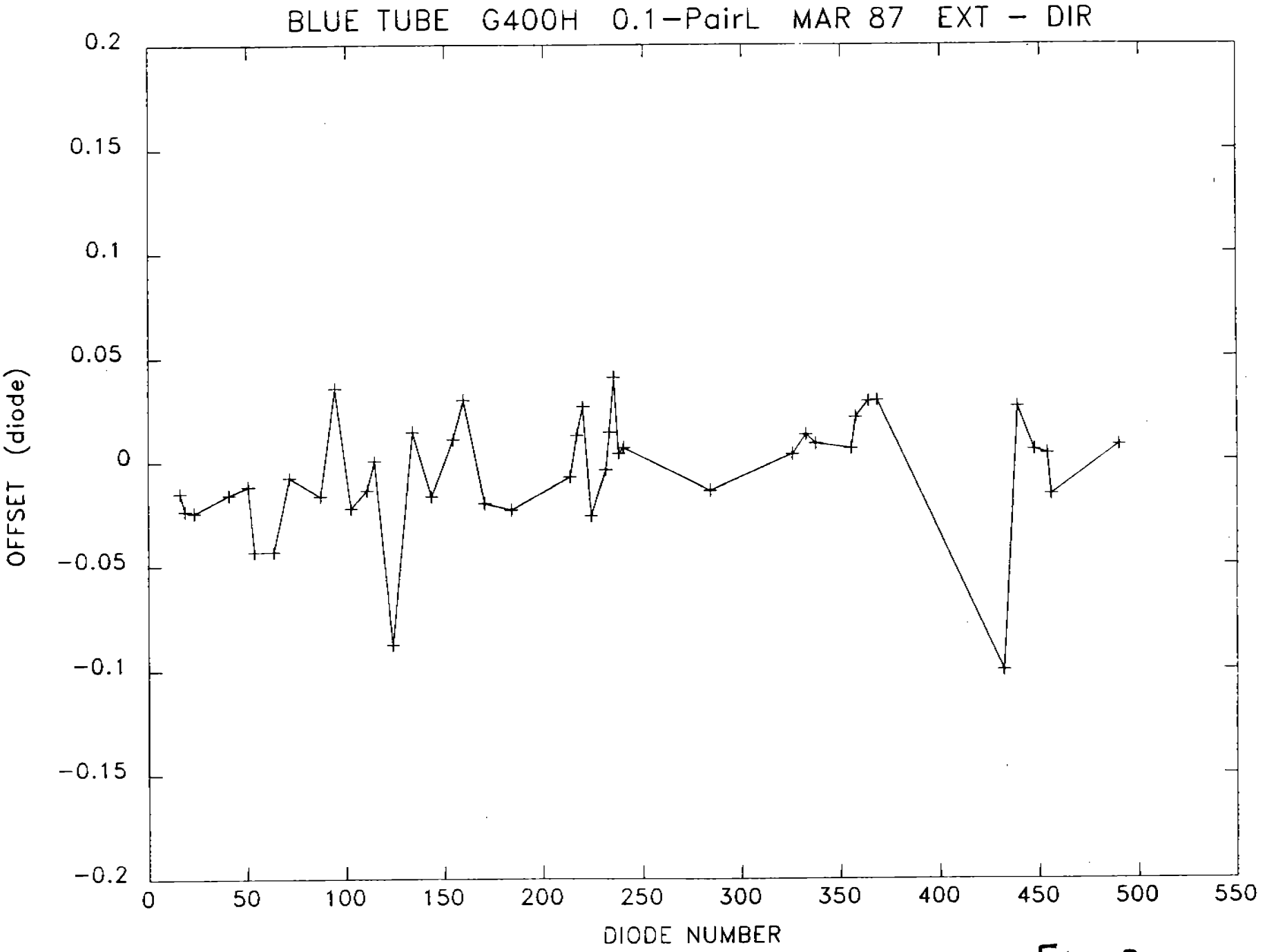
BLUE TUBE G400H 0.1-PairL MAR 87 EXT - DIR
0.2
0.15
0.1
0.05
0
-0.05
-0.1
-0.15
-0.2
OFFSET (diode)
0
50
100
150
200
250
300
350
400
450
500
550
DIODE NUMBER

Fig. 3a

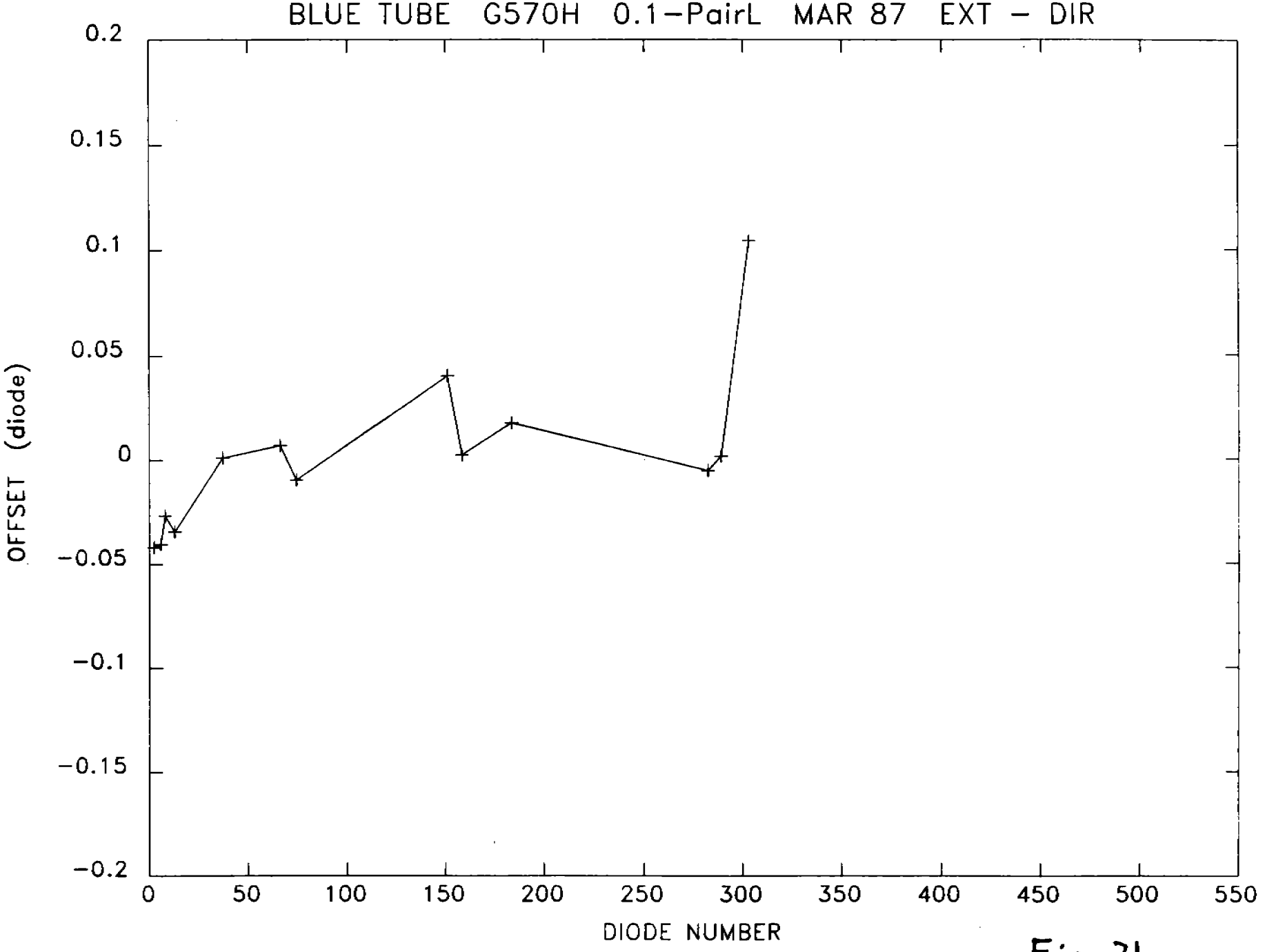
BLUE TUBE G570H 0.1-PairL MAR 87 EXT - DIR
0.2
0.15
0.1
0.05
0
-0.05
-0.1
-0.15
-0.2
OFFSET (diode)
0
50
100
150
200
250
300
350
400
450
500
550
DIODE NUMBER

Fig. 3h

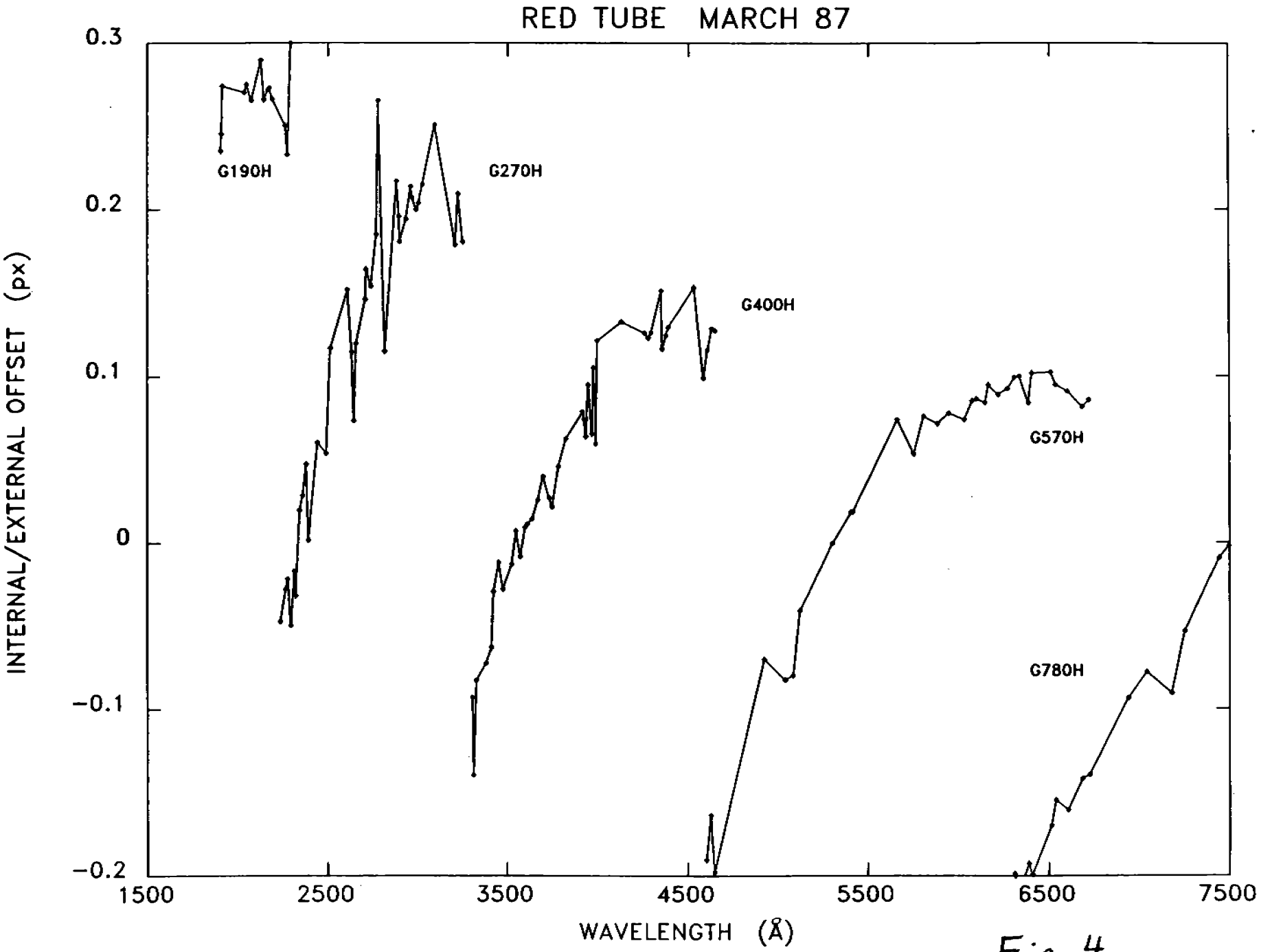
RED TUBE MARCH 87
INTERNAL/EXTERNAL OFFSET (px)
0.3
0.2
0.1
0
−0.1
−0.2
G190H
G270H
G400H
G570H
G780H
1500
2500
3500
4500
5500
6500
7500
WAVELENGTH (Å)

Fig. 4

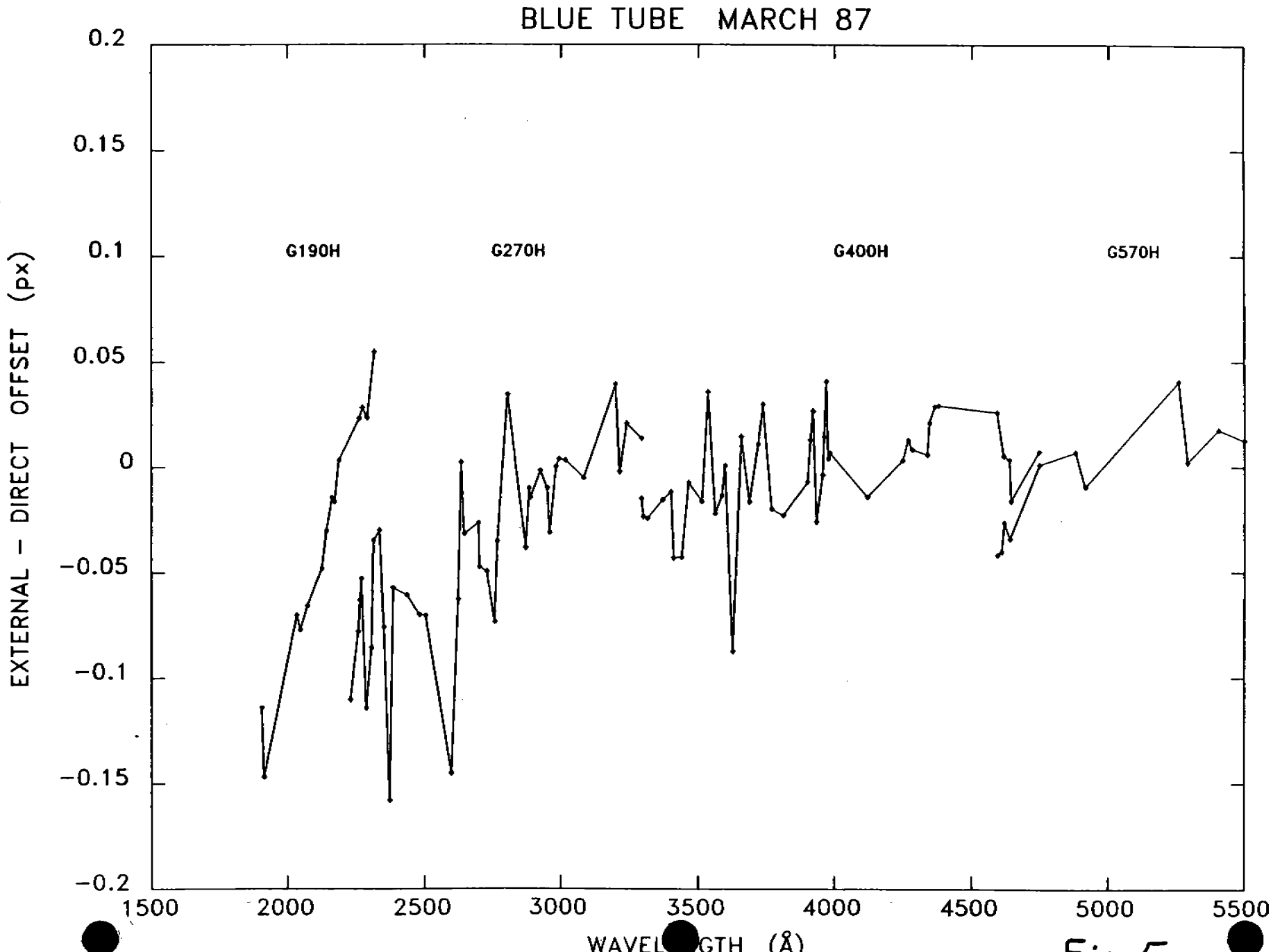
BLUE TUBE MARCH 87
G190H
G270H
G400H
G570H
EXTERNAL - DIRECT OFFSET (px)
0.2
0.15
0.1
0.05
0
−0.05
−0.1
−0.15
−0.2
1500
2000
2500
3000
3500
4000
4500
5000
5500
WAVEL GTH (Å)

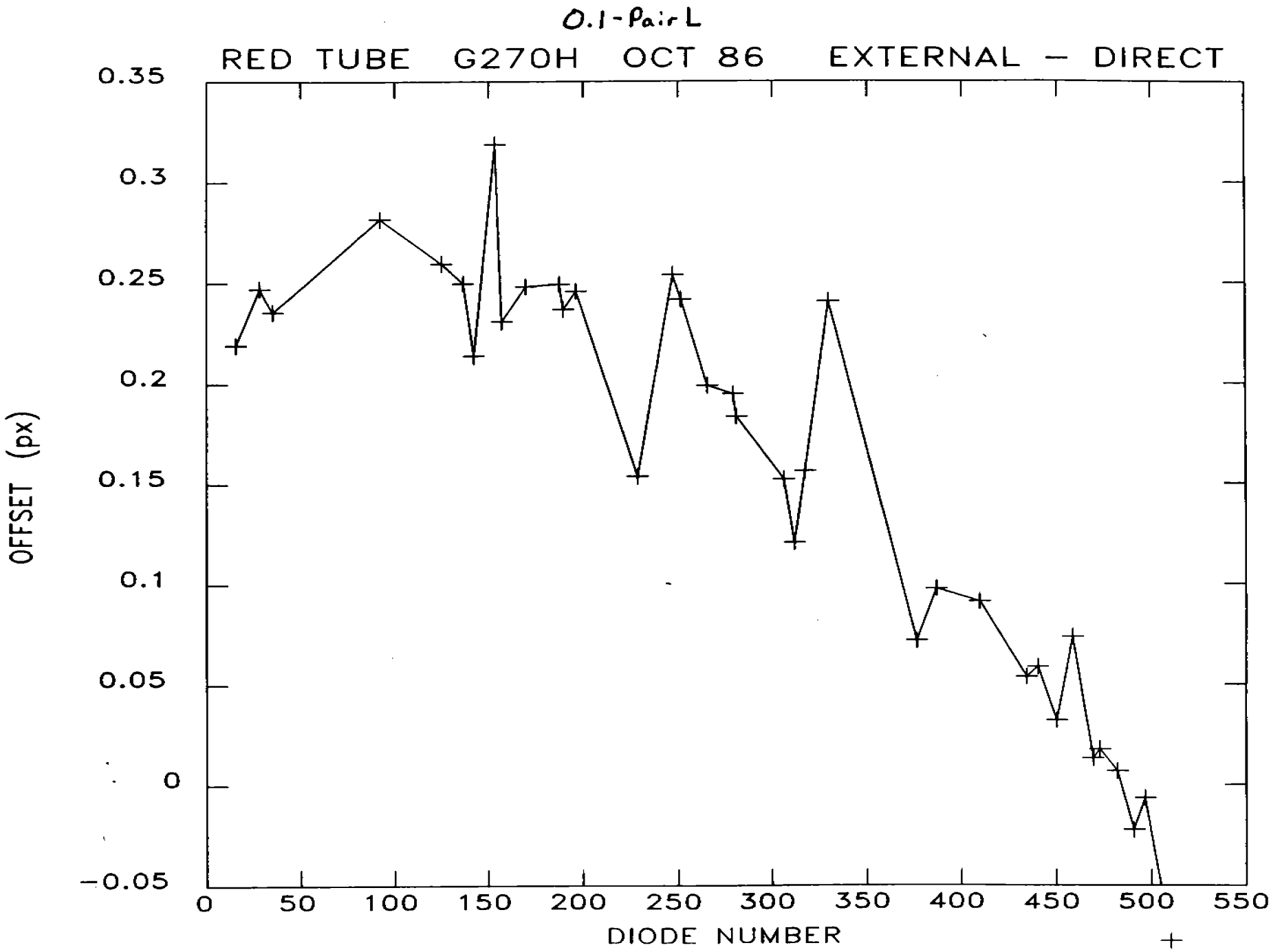
0.1-Pair L
RED TUBE G270H OCT 86 EXTERNAL – DIRECT
OFFSET (px)
0.35
0.3
0.25
0.2
0.15
0.1
0.05
0
−0.05
0
50
100
150
200
250
300
350
400
450
500
550
DIODE NUMBER

Fig. 6

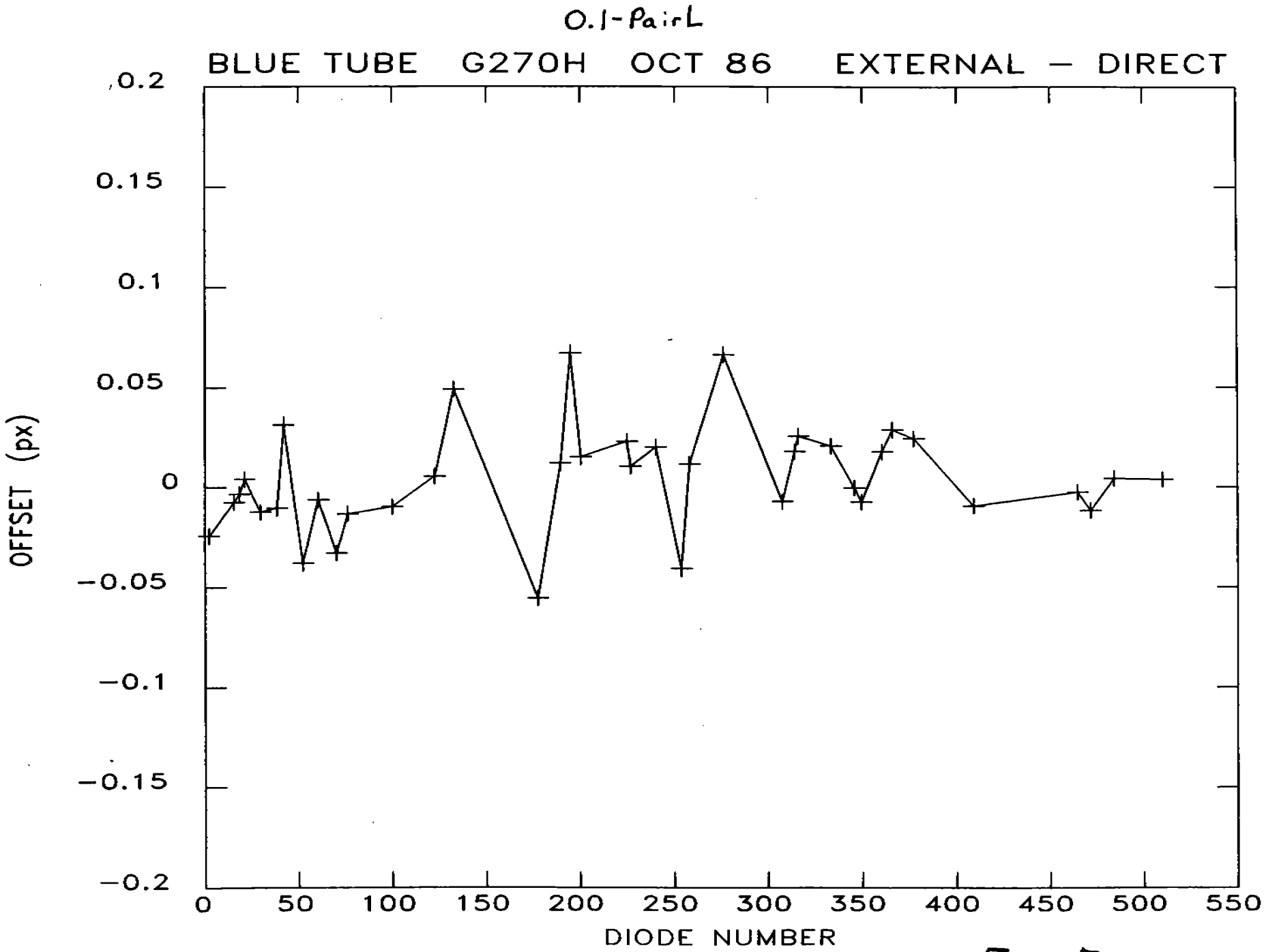
0.1-PairL
BLUE TUBE G270H OCT 86 EXTERNAL – DIRECT
0.2
0.15
0.1
0.05
0
−0.05
−0.1
−0.15
−0.2
OFFSET (px)
0
50
100
150
200
250
300
350
400
450
500
550
DIODE NUMBER

Fig. 7

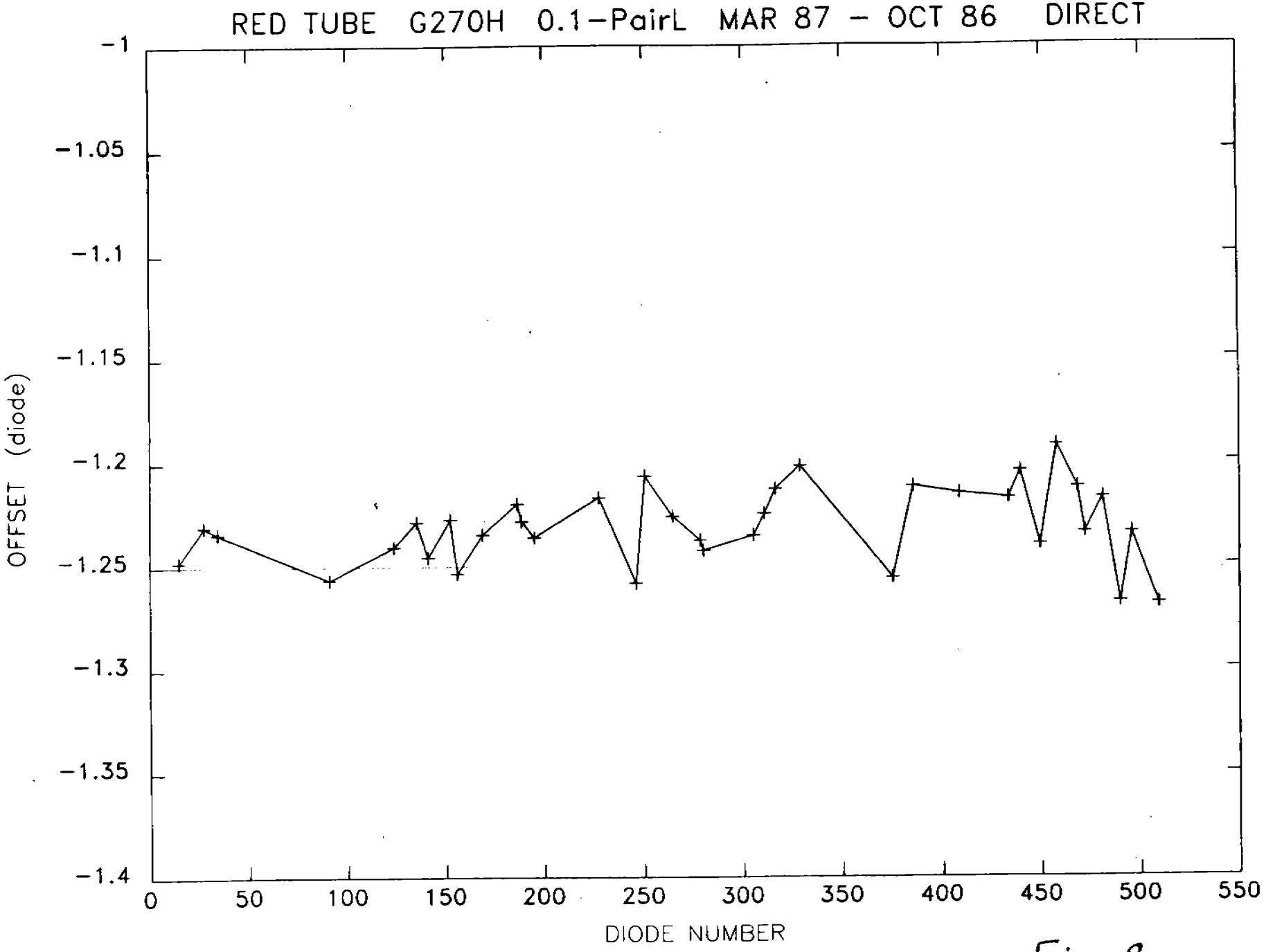
RED TUBE G270H 0.1-PairL MAR 87 - OCT 86 DIRECT
OFFSET (diode)
-1
-1.05
-1.1
-1.15
-1.2
-1.25
-1.3
-1.35
-1.4
0
50
100
150
200
250
300
350
400
450
500
550
DIODE NUMBER

Fig. 8a

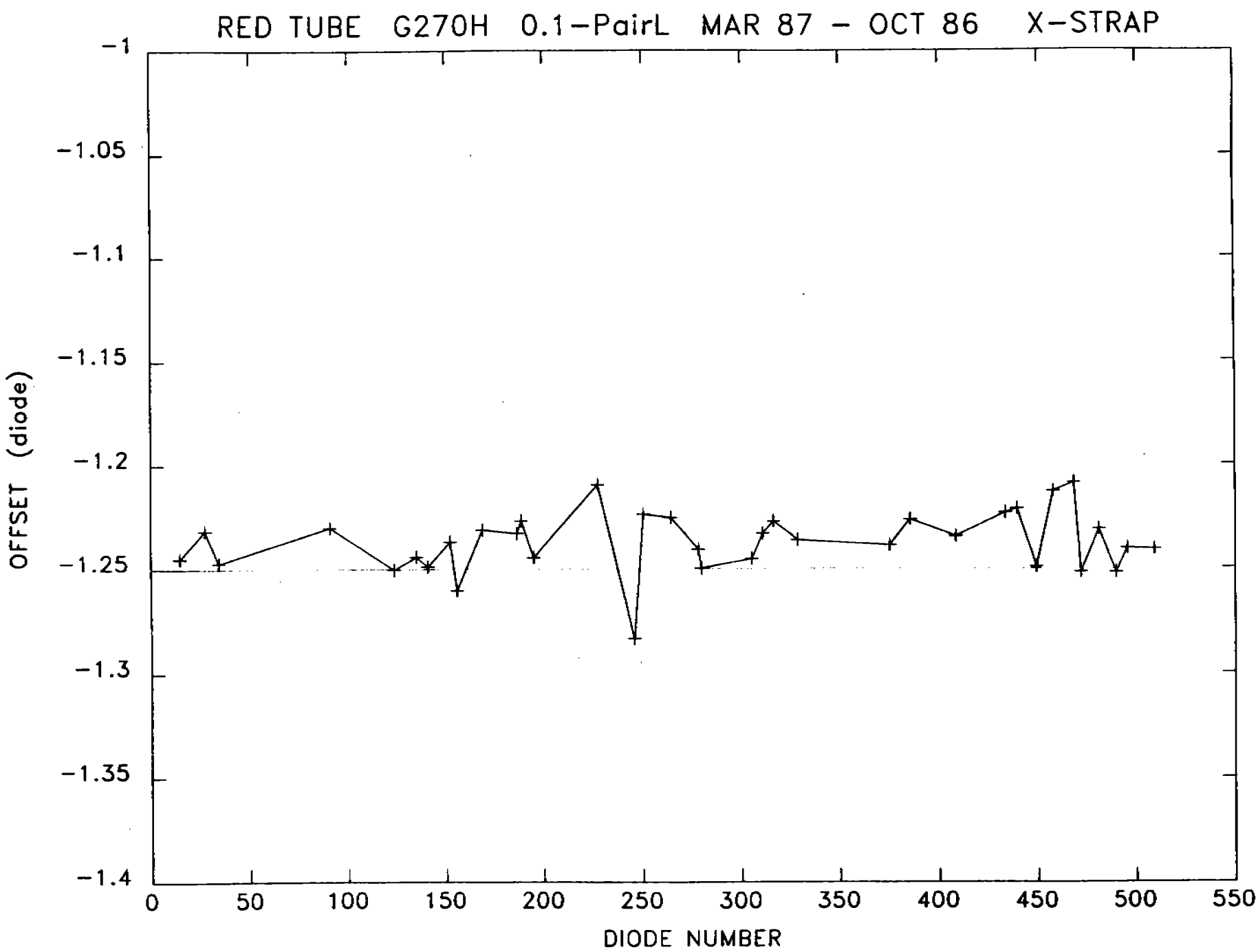
RED TUBE G270H 0.1-PairL MAR 87 - OCT 86 X-STRAP
OFFSET (diode)
-1
-1.05
-1.1
-1.15
-1.2
-1.25
-1.3
-1.35
-1.4
0
50
100
150
200
250
300
350
400
450
500
550
DIODE NUMBER

Fig. 8b

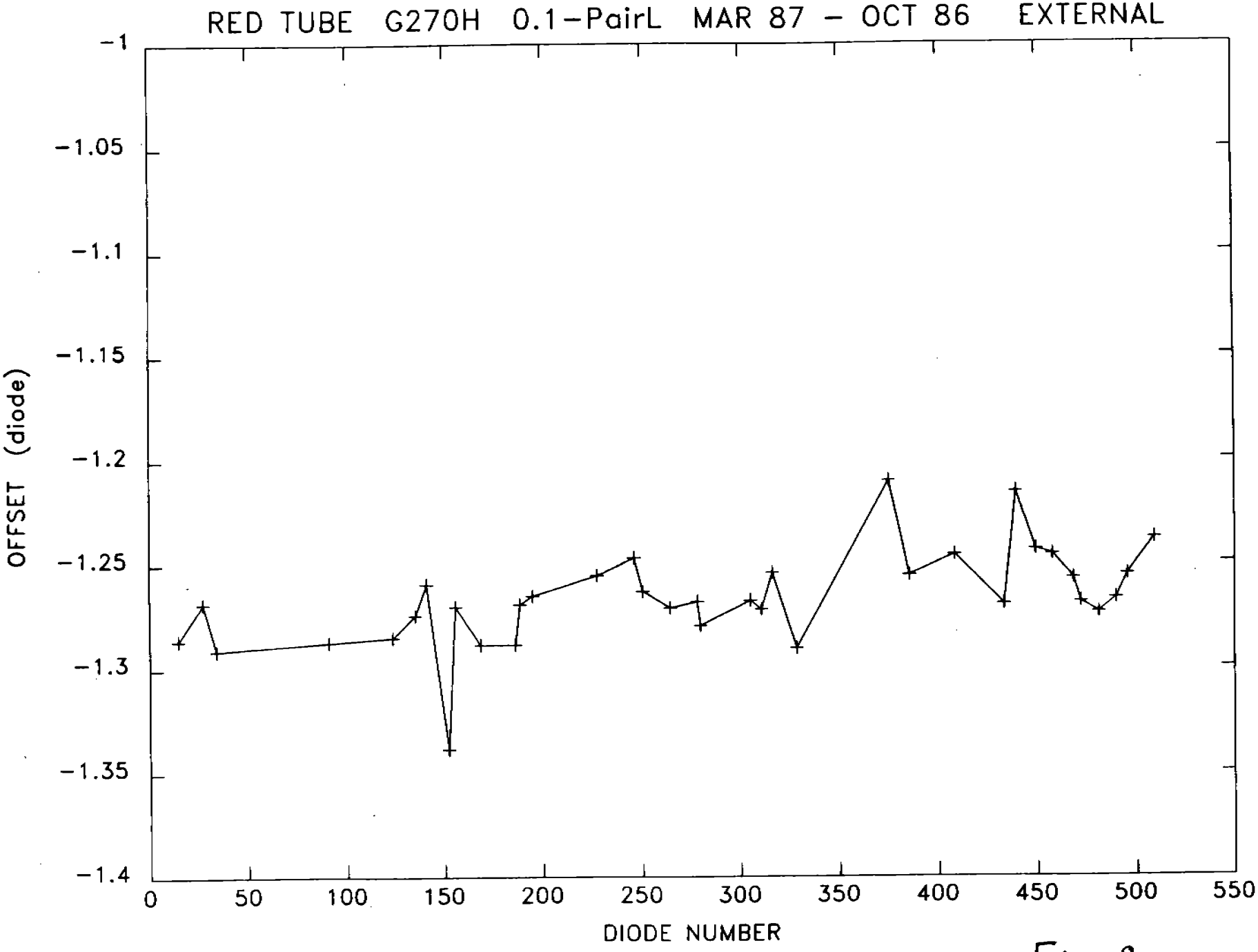
RED TUBE G270H 0.1-PairL MAR 87 - OCT 86 EXTERNAL
OFFSET (diode)
-1
-1.05
-1.1
-1.15
-1.2
-1.25
-1.3
-1.35
-1.4
0
50
100
150
200
250
300
350
400
450
500
550
DIODE NUMBER

Fig. 8c

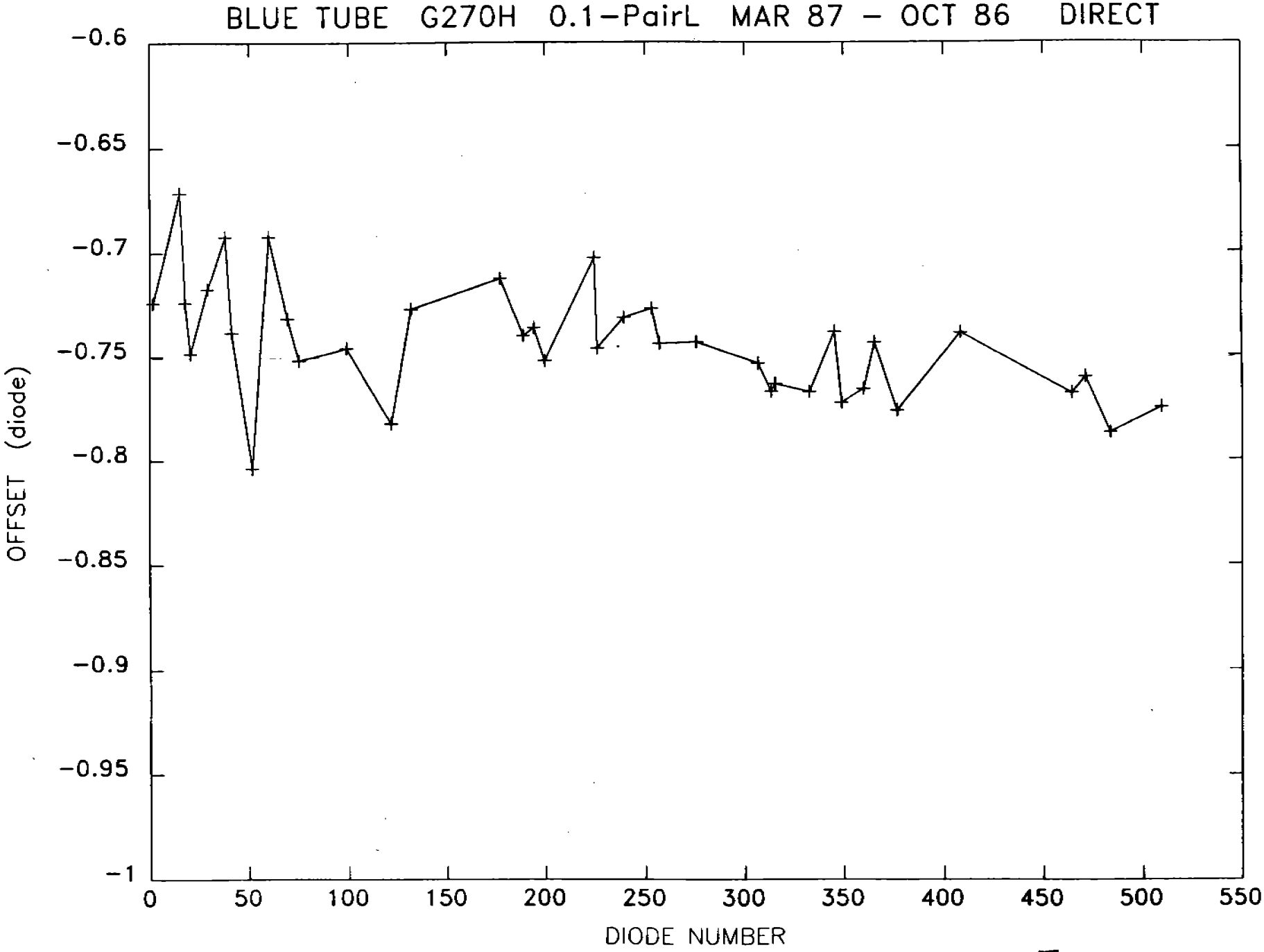
BLUE TUBE G270H 0.1-PairL MAR 87 - OCT 86 DIRECT
OFFSET (diode)
-0.6
-0.65
-0.7
-0.75
-0.8
-0.85
-0.9
-0.95
-1
0
50
100
150
200
250
300
350
400
450
500
550
DIODE NUMBER

Fig. 9a

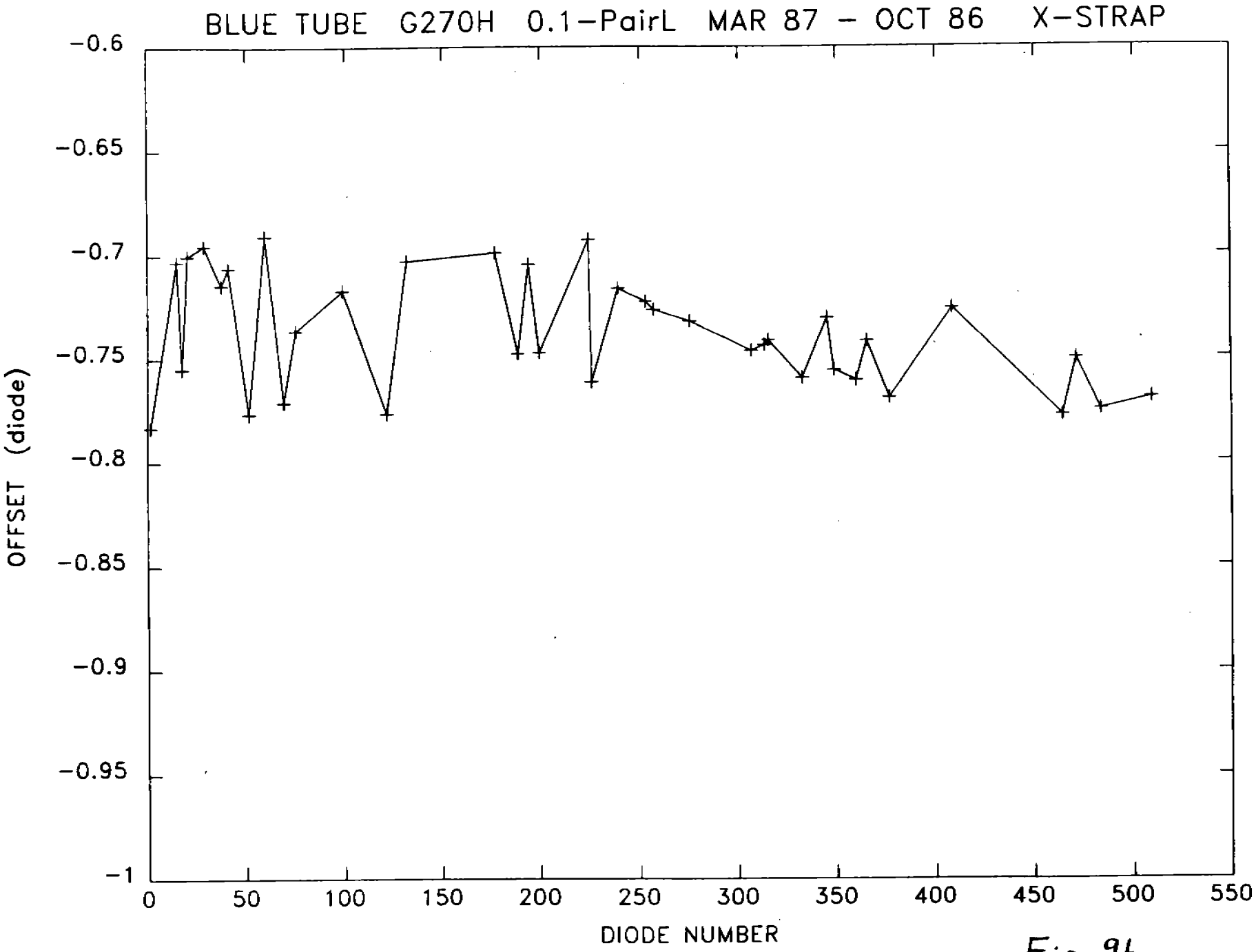
BLUE TUBE G270H 0.1-PairL MAR 87 - OCT 86 X-STRAP
OFFSET (diode)
-0.6
-0.65
-0.7
-0.75
-0.8
-0.85
-0.9
-0.95
-1
0
50
100
150
200
250
300
350
400
450
500
550
DIODE NUMBER

Fig. 96

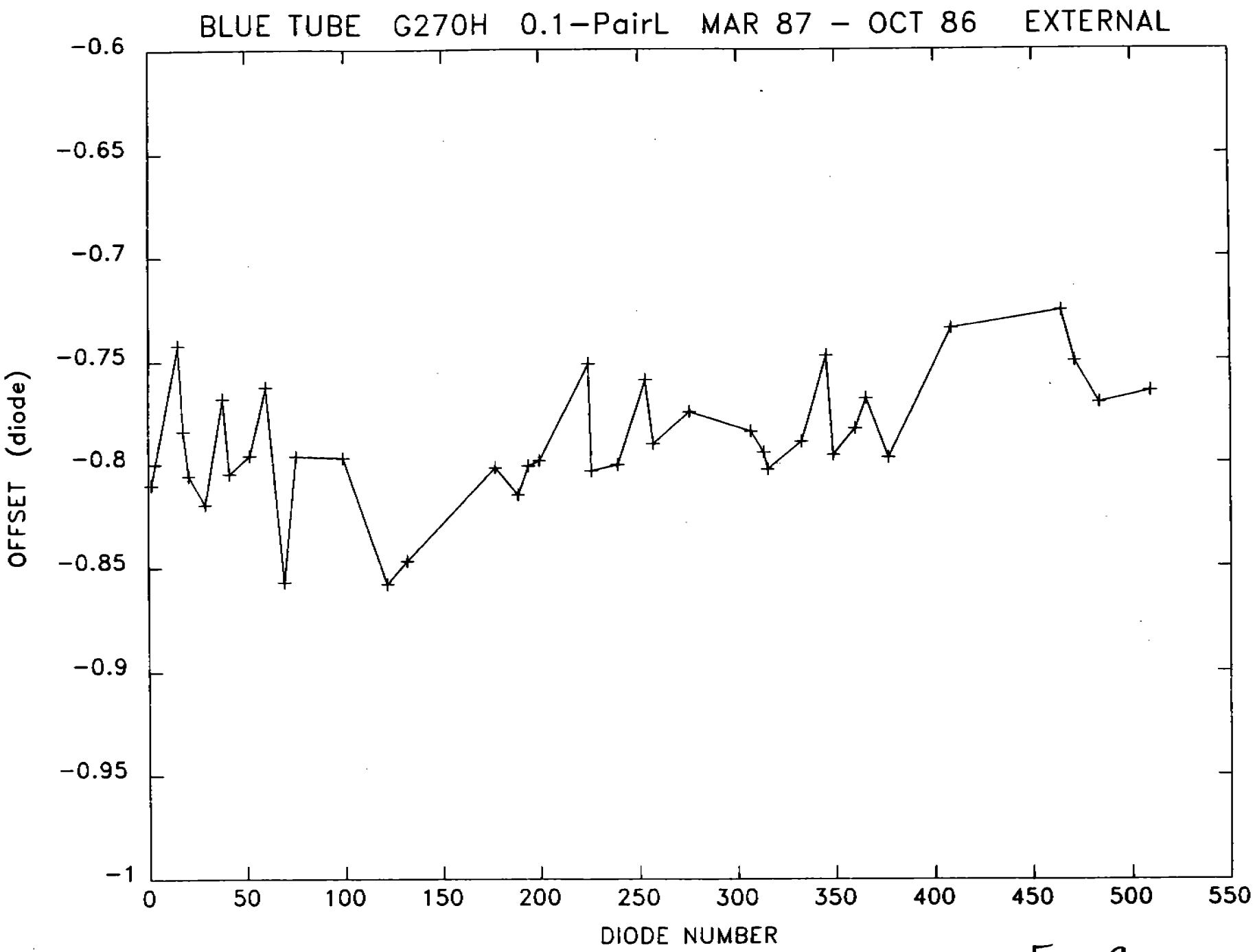
BLUE TUBE G270H 0.1-PairL MAR 87 - OCT 86 EXTERNAL
OFFSET (diode)
-0.6
-0.65
-0.7
-0.75
-0.8
-0.85
-0.9
-0.95
-1
0
50
100
150
200
250
300
350
400
450
500
550
DIODE NUMBER

Fig. 9c

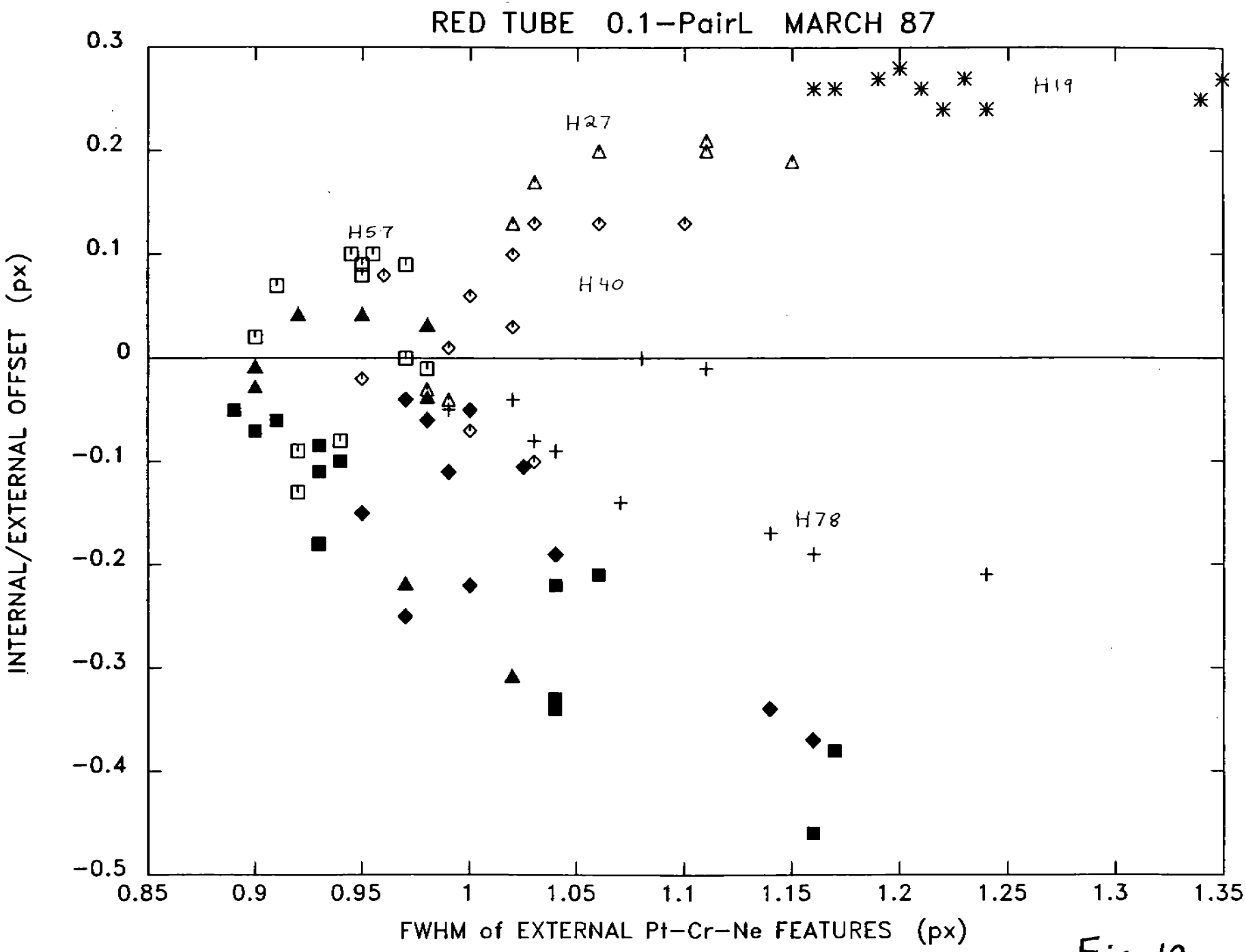
RED TUBE 0.1-PairL MARCH 87
INTERNAL/EXTERNAL OFFSET (px)
FWHM of EXTERNAL Pt-Cr-Ne FEATURES (px)
0.3
0.2
0.1
0
-0.1
-0.2
-0.3
-0.4
-0.5
0.85
0.9
0.95
1
1.05
1.1
1.15
1.2
1.25
1.3
1.35
H19
H27
H57
H40
H78

Fig. 10